Copy No. 29

NASA General Working Paper No. 10,014

PRINCIPLES AND APPLICATION OF SHOCK TUBES AND SHOCK TUNNELS

DISTRIBUTION AND REFERENCING

NATIONAL AERONAUTICS AND SPACE ADMINISTRATION
MANNED SPACECRAFT CENTER
Houston, Texas
October 22, 1963

NASA General Working Paper No. 10,014

PRINCIPLES AND APPLICATION OF SHOCK TUBES AND SHOCK TUNNELS

Prepared by: Robert C Ried
Robert C. Ried
AST, Fluid and Flight Mechanics

for Robert C Ried
Harry G. Clauss, Jr.
Cooperative Student

Authorized for Distribution

Warren Gillespie, Jr.
for Maxime A. Faget
Assistant Director for Engineering and Development

NATIONAL AERONAUTICS AND SPACE ADMINISTRATION

MANNED SPACECRAFT CENTER

HOUSTON, TEXAS

October 22, 1963

I

TABLE OF CONTENTS

LIST OF FIGURES

PRINCIPLES AND APPLICATION OF SHOCK TUBES AND SHOCK TUNNELS

ABSTRACT

The principles, theoretical flow equations, calculation techniques, limitations and practical performance characteristics of basic and high performance shock tubes and shock tunnels are presented. Selected operating curves are included.

SUMMARY

The basic shock tube flow is a transient response to an initial pressure discontinuity. An investigation of the theoretical flow equations indicates that the performance of a shock tube is extended as the driver gas speed of sound is increased. In addition, within the limitations of a reasonable source of energy for a shock tube, a variable area shock tube has many advantages. The high performance shock tube is limited by diminishing returns and practical aspects of the flow, such as the available test time.

A shock tunnel is a nozzle which utilizes the stagnation conditions created by a shock tube. The shock tunnel is useful from a Mach number, Reynolds number standpoint, while the shock tube has a high capability in enthalpy and pressure.

INTRODUCTION

Aerothermodynamic problems associated with earth reentry have stimulated rather extensive research in high temperature gases. The inherent complexity of the associated chemistry, physics, and gas dynamics problems has required considerable experimental effort.

To achieve an insight into the fundamental and operational aspects of advanced gas dynamic facilities the characteristics and limitations of simple and high performance shock tubes and shock tunnels have been investigated. It is hoped that this investigation will enable an insight into the optimum use of ground facilities.

SYMBOLS

A	cross sectional area of tube
a	speed of sound
C_p	specific heat at constant pressure
C_v	specific heat at constant volume
$\frac{\Delta E}{v}$	electrical discharge energy per unit volume of driver gas

F_{tu}	ultimate tensile stress
h	enthalpy
L	length of driven chamber
M	Mach number, $\frac{U}{a}$
p	pressure
RT_o	reference enthalpy, 33.86 $\frac{Btu}{lb_m}$
S	entropy
T	temperature
t	tube wall thickness
U	velocity
x	distance along driven chamber starting at the diaphragm, x = 0
γ	ratio of specific heats, $\frac{C_p}{C_v}$
η	overall efficiency of electrical discharge process
θ	time
μ	viscosity
ρ	density
τ	test time

Subscripts

1	initial, undisturbed driven gas (fig. 1)
2	shocked driven gas (fig. 1)
3	expanded driver gas (fig. 1)
4	initial, undisturbed driver gas (fig. 1)

5	reflected test gas (figs. 1 and 21)
6	expanded test gas (fig. 21)
c.s.	contact surface
r.s.	reflected shock
s	incident normal shock
t	total or stagnation state
∞	free stream conditions encountered in flight

Superscripts

'	constant area shock tube conditions
*	nozzle throat conditions

DISCUSSION

Shock Tubes

The shock tube is one of the most versatile and useful experimental apparatus ever devised. The extreme range of conditions that may be obtained in a shock tube lend its uses from the pure research by physicists or chemists to simulation for engineers.

Principle of operation.- The operation of a shock tube may be illustrated by considering a constant diameter tube divided into two regions by a diaphragm as illustrated in figure 1(a). A gas pressure difference is established across the diaphragm. The higher pressure region is called the driver chamber while the lower pressure region is the driven chamber. In operation, the diaphragm is burst either by creating a pressure difference which exceeds the strength of the diaphragm or by initiating the opening by a puncture. This allows the driver gas to expand into the driven chamber. The flow regions in the shock tube are shown as functions of time and their position in the shock tube in figure 1(b). The use of such a figure is particularly convenient in describing the transient processes in the shock tube. It should be noted that the reciprocal of the slopes of lines in this figure are indicative of velocities. The following sections describe the gas dynamic processes occurring in the shock tube.

Normal shock wave: Following the diaphragm burst, the expanding driver gas behaves much like a piston as it propagates into the driven chamber. The driver gas accelerates and compresses the driven gas in a manner that initially produces a strong pressure gradient between the compressed and the undisturbed driven gas. This pressure gradient rapidly develops into a compression or shock wave which propagates into the driven gas ahead of the expanding driver gas as shown in figure 1(b). Once the shock wave is formed it becomes the mechanism of accelerating, compressing and heating the driven gas. Since the undisturbed driven gas is at rest, the velocity of the shock wave is fixed by the strength of the shock $\left(\frac{P_2}{P_1}\right)$. The strength of the shock wave is maintained by the expansion of the driver gas. Specifically, the driven gas is compressed to a pressure $\left(P_2\right)$ that is equal to the pressure $\left(P_3\right)$ to which the driver gas has expanded. This is illustrated schematically in figure 1(c) where the pressure distribution within the shock tube is shown at one instant of time after diaphragm rupture.

Although the velocity of the shock wave is roughly constant, the overall shock tube flow might best be considered as the transient process of the initial driver and driven gases approaching an intermediate equilibrium state.

The contact surface and test gas: The interface between the driver and driven gas is termed the contact surface. By definition there is no mass flux across this surface, and from continuity considerations the pressure and velocity on both sides must be equal. There can be significant temperature and density discontinuities across the contact surface. As an example, figure 1(d) illustrates a possible temperature distribution throughout the shock tube, at the selected time.

The gas between the shock wave and the contact surface is termed the test gas. This gas may simulate the gas between a blunt entry vehicle and the bow shock wave. The temperature, pressure, velocity, et cetera, may correspond to full scale flight conditions. The contact surface becomes effectively the blunt face of the full scale vehicle. Thus for the simulation of a normal shock at flight conditions a shock tube does not require a model in the flow. The problem of scaling real gas effects with vehicle size does not occur.

The driver gas expansion: Path lines have been included in figure 1(b) to illustrate the flow of the driver and driven gases. It should be noted that the expansion of the driver gas is not a discontinuous process as the shock wave, but rather the driver gas accelerates from rest to the expanded driver gas velocity in the form of an expansion

fan. The expansion fan converts the stagnation energy of the driver gas into the flow energy of the expanded driver gas and the work done in compressing and accelerating the driven gas. The incremental expansion waves, composing the expansion fan, travel at the speed of sound relative to the local driver gas conditions. Thus the driver gas speed of sound determines the maximum integrated rate at which the driver gas stagnation energy may be converted to the expanded driver gas kinetic energy, or the rate and proportion of work used in compressing the driven gas. Although the driver gas expansion is an unsteady process, if the flow is assumed invicid, the expanded driver gas pressure (P_3), the pressure behind the shock ($P_2 = P_3$), and the shock velocity are all constant.

Analysis of shock tube flows: A quantitative analysis of the primary flow in a shock tube combines the normal shock wave relations, applied to the driven gas and relative to the shock wave, with the unsteady isentropic expansion of the driver gas. These relations are matched at the contact surface where the pressures and velocities must be respectively equal, as previously mentioned. The general shock tube flow relations for a perfect gas have been derived in detail in many excellent papers (for example, refs. 1 and 2), and the derivations will not be reproduced here.

Ideal gas relation: The flow in a constant area shock tube is completely determined by the driver and driven gases and their thermodynamic states. For ideal gases the thermodynamic properties may be made dimensionless by the ratio of the driver gas property to the corresponding driven gas property. For a pressure driven shock tube the flow parameters may be expressed as a function of the initial driver to driven gas pressure ratio $\left(\frac{P_4}{P_1}\right)$.

Since a shock, or compression, wave is the propagation of a discontinuity in pressure, the pressure ratio across the shock is termed the shock strength. In the case of the shock tube the strength of the shock wave $\left(\frac{P_2}{P_1}\right)$ is related to the initial pressure ratio in the following way (ref. 2).

$$\frac{P_4}{P_1} = \frac{P_2}{P_1}\left[1 - \left(\frac{P_2}{P_1} - 1\right)\sqrt{\frac{\left(\frac{\gamma_4 - 1}{2\gamma_4}\right)\frac{C_{v1}\,T_1}{C_{v4}\,T_4}}{\left(\frac{\gamma_1 + 1}{\gamma_1 - 1}\right)\frac{P_2}{P_1} + 1}}\right]^{\frac{2\gamma_4}{1 - \gamma_4}} \qquad (1)$$

The subscripts in all of the relations refer to the regions outlined in figure 1(b).

The ideal gas relations for additional shock tube flow parameters may be simplified considerably by expressing them as a function of the shock strength as obtained from equation (1). For example, the shock front Mach number or velocity may be expressed as:

$$M_s = \frac{U_s}{a_1} = \left\{ \frac{\gamma_1 - 1}{2\gamma_1} \left[1 + \frac{P_2}{P_1} \left(\frac{\gamma_1 + 1}{\gamma_1 - 1} \right) \right] \right\}^{\frac{1}{2}} \tag{2}$$

It is to be noted that for a strong shock $\left(\text{large } \frac{P_2}{P_1} \right)$ the shock front Mach number is roughly proportional to the square root of the shock strength. The Mach number of the test gas, however,

$$M_2 = \frac{U_2}{a_2} = \frac{\left(\frac{P_2}{P_1} - 1 \right)}{\gamma_1} \left[\frac{\gamma_1 - 1}{2\gamma_1} \left(\frac{P_2}{P_1} \right) \left(\frac{\gamma_1 + 1}{\gamma_1 - 1} + \frac{P_2}{P_1} \right) \right]^{-\frac{1}{2}} \tag{3}$$

approaches a constant value for strong shocks. The reason for this phenomena is that although the test gas velocity,

$$U_2 = \frac{a_1}{\gamma_1} \left(\frac{P_2}{P_1} - 1 \right) \left\{ \frac{\gamma_1 - 1}{2\gamma_1} \left[\left(\frac{\gamma_1 + 1}{\gamma_1 - 1} \right) \frac{P_2}{P_1} + 1 \right] \right\}^{-\frac{1}{2}} \tag{4}$$

increased with the square root of the shock strength for strong shocks, so does the speed of sound in the test gas,

$$a_2 = a_1 \left[\frac{\frac{P_2}{P_1} \left(\frac{\gamma_1 + 1}{\gamma_1 - 1} + \frac{P_2}{P_1} \right)}{1 + \left(\frac{\gamma_1 + 1}{\gamma_1 - 1} \right) \frac{P_2}{P_1}} \right]^{\frac{1}{2}} \tag{5}$$

In an effort to obtain high Mach number shocks and therefore greater shock strengths, it is of interest to note that for large initial pressure ratios and strong shocks the shock strength may be obtained from equation (1) in the approximate form,

$$\frac{P_2}{P_1} \simeq \frac{2\,\gamma_1\left(\gamma_1 + 1\right)}{\left(\gamma_4 - 1\right)^2}\left(\frac{a_4}{a_1}\right)^2 \tag{6}$$

This relation indicates that the strength of the shock will increase for an increase in the driver gas speed of sound or a decrease in the driver gas ratio of specific heats. Unfortunately, a gas with a low ratio of specific heats will tend toward a high molecular weight and thus a lower speed of sound for a given temperature. Thus, to obtain strong or high Mach number shocks, it is desirable to use a low molecular weight driver gas at a relatively high temperature. This is in agreement with the previous qualitative discussion in that the driver gas speed of sound determines the limit for the rate at which the driver gas stagnation energy is converted into kinetic energy.

Real gas computations: In considering the flow of a real gas in a shock tube, it is necessary to replace the caloric equation of state used in the derivation of the ideal gas relations by the equilibrium properties of the gas. For a given driver gas state and a given driven gas temperature (ambient temperature) the flow parameters may be calculated in the following manner.

If the expansion of the driven gas is assumed to be isentropic, the unsteady energy equation (ref. 3),

$$\left(\frac{dh}{a}\right)_s + du = 0 \tag{7}$$

may be integrated graphically in the following form.

$$u_3 = -\int_4^3 \left(\frac{1}{a}\right) dh_s \tag{8}$$

The expanded driver gas state, state 3, is uniquely determined by the assumption of constant entropy ($S_3 = S_4$) and the selection of the expanded

pressure (P_3). Thus, the pressure and velocity of the test gas are fixed by the contact surface restrictions,

$$P_3 = P_2 \tag{9a}$$

$$U_3 = U_2 \tag{9b}$$

At this point one property of the test gas has been fixed (P_2) and one property of the driven gas has been fixed (T_1). The remainder of the calculation is an iterative process utilizing the boundary condition of the test velocity, U_2. If the driven gas state is selected, the enthalpy of the test gas may be obtained from

$$h_2 = h_1 + \frac{P_2 - P_1}{\rho_1} - \frac{U_2^2}{2} \tag{10}$$

The enthalpy and the pressure of the test gas fix the thermodynamic state. The test gas density may be obtained from the equilibrium properties of the gas. If the state of the driven gas that has been selected is correct, the density obtained above will agree with the following relation.

$$\rho_2 = \frac{P_2 - P_1}{h_2 - h_1 - \frac{U_2^2}{2}} \tag{11}$$

Once the correct driven gas state is determined the shock velocity

$$U_s = \frac{P_2 - P_1}{\rho_1 U_2} \tag{12}$$

may be obtained.

Ideal driver gas, real driven gas: In certain phases of shock tube operation, an inert, monatomic driver gas is used. For these cases, it is many times possible to assume that the driver gas behaves as an ideal gas. This simplifies the calculation procedure in that the graphical integration procedure required for the real gas is no longer required.

If the driven gas state and the shock speed, U_s, are selected, the density of the test gas may be expressed as a function of the test gas pressure,

$$\rho_2 = \frac{\rho_1^2 U_s^2}{P_1 - P_2 + \rho_1 U_s^2} \tag{13}$$

By assuming a value of the test gas pressure, P_2, the test gas density may be calculated from equation (13). Thus, having two properties of the test gas, $(P_2\ \rho_2)$, the enthalpy is determined by the equilibrium properties of the test gas. If the test gas pressure assumed is correct, this enthalpy will agree with the energy equation,

$$h_2 = h_1 + \frac{P_2 - P_1}{\rho_1} - \frac{\left(P_2 - P_1\right)^2}{2\rho_1^2 U_s^2} \tag{14}$$

When the correct test gas pressure is obtained the test gas velocity,

$$U_2 = \frac{P_2 - P_1}{\rho_1 U_s} \tag{15}$$

may be obtained directly.

The properties behind a normal shock have been tabulated as a function of the initial state and the shock velocity for air (refs. 4 and 5). This, of course, eliminates the need for the previous iteration process.

In either case, relations for the isentropic expansion of an ideal driver gas may be obtained by integration of the simple wave relations across the expansion fan. Thus the initial driver pressure

$$P_4 = P_2 \left(1 - \frac{U_2\left(\gamma_4 - 1\right)}{2\ a_4}\right)^{\frac{2\ \gamma_4}{1 - \gamma_4}} \tag{16}$$

may be obtained directly for any given a_4 and γ_4 and for the test

gas pressure (P_2) and velocity (U_2) required. Since the speed of sound in the driver gas (a_4) and the driver pressure (P_4) are known, the driver gas state is determined.

Performance characteristics.- To illustrate the magnitudes of the shock tube flow parameters under various conditions, the results for a pressure driven, constant area shock tube are presented in figures 2 through 6. Consideration is given to the use of air as the driver and driven gases and to helium as the driver gas with air in the driven chamber. In addition, the results of two sets of calculations for heated helium driver gas and air driven gas are given. The initial helium driver gas temperatures used are T_4 = 31, 175° R and 15,848° R.

These calculations are presented under the assumption of ideal gases and also with the considerations of real air. Since helium is relatively inert up to temperatures of the order of 15,000° K where ionization becomes significant, it has been considered as an ideal gas.

Shock strength: For ideal gases the shock strength may be determined as a function of the initial pressure ratio by the use of equation (1). This relation is plotted in figure 2 for the four cases considered. The range of operation and the maximum shock strength obtainable increase greatly in considering the use of helium as the driver gas in comparison with air, or in considering the use of heated helium driver gas as compared to room temperature helium.

The real air calculations appear to be in reasonable agreement with the ideal gas relations; however, to obtain a given shock strength using heated helium and real air the calculations indicate that the initial pressure ratio required can easily be 30 percent greater than that given by the ideal gas relations.

In addition, the hypothetical maximum shock strength for ideal helium driver gas and ideal air driven gas is shown as a function of the initial pressure ratio. It is to be noted that the shock strength approaches the initial pressure ratio. This is to be expected since, as the driver gas temperature approaches infinity, the speed of sound in the driver gas also approaches infinity, and this determines the rate at which the stagnation energy of the driver gas is dissipated.

Shock Mach number and velocity: Equation (2) is the relation between the shock Mach number or velocity and the shock strength for ideal gases. These relations are shown respectively in figures 3 and 4 for the four cases considered. It is to be noted that the shock Mach numbers and velocities realized with real air are generally somewhat lower than the ideal gas predictions. It does appear, however, that

using heated helium driver gas, a shock velocity of 35,000 feet per second could be obtained with a reasonable initial pressure ratio on the order of 10^5.

The maximum Mach number and shock velocity are also shown in these figures. The maximum values indicate that the initial pressure ratio must be high for a high performance shock tube. This was assumed in equation (6) where the attempt was to determine the parameters of importance for high performance. At this point, it can be concluded that the high performance requirements for a shock tube are a high initial pressure ratio and a high driver gas speed of sound.

Test gas velocity and Mach number: Figures 5 and 6 show, respectively, the test gas velocity and Mach number as a function of the initial pressure ratio for the cases considered. The test gas velocity for the real air calculations agrees reasonably well with the ideal gas relations. The Mach number, however, varies considerably under the assumptions of real or ideal air. The main reason for this difference is due to the temperature in the test gas. As the shock Mach number increases, the enthalpy of the test gas increases. In real air, chemical and thermodynamic modes of freedom absorb some of this enthalpy and thus result in a lower overall temperature when compared to an ideal gas. The effect increases with increasing enthalpy or temperature. This is supported in figure 6 where the disagreement increases with initial pressure ratio and or shock Mach number.

Electric driver.- Both of the heated helium driver gas sample calculations indicate that this mode of operation would at least theoretically cover an operating range which includes significant ionization of air. There is, however, a practical problem of obtaining and maintaining the driver gas stagnation conditions. Since the heat lost by thermal radiation is roughly proportional to at least the fourth power of the temperature, a high temperature driver gas will rapidly cool by radiation heat transfer alone. It is desirable, therefore, to heat the driver gas instantaneously before the diaphragm is burst. This mode of heating is also desirable from the standpoint of the driver chamber strength requirements. The driver gas would be cooled by the expansion fan before the chamber temperature would be increased significantly.

Although a combustible driver gas will meet the requirements of an almost instanteous energy source, the products of combustion necessarily have a higher molecular weight than helium. Thus, at a given temperature, the speed of sound in the products of combustion is correspondingly less than that of helium. Although hydrogen has a lower molecular weight than helium, hydrogen absorbs a considerable amount of energy by dissociation. In addition, hydrogen will react at the contact surface and presents an overall safety hazard.

It appears that the most reliable, economic, and efficient method for rapidly heating helium to extremely high enthalpies is by the discharge of an electric arc through the driver chamber. The potential for the arc may be obtained by the use of a capacitor bank, and the arc may be initiated by the use of a small diameter starter wire. Figures 7 through 9 illustrate the stagnation properties of helium as a function of the arc discharge energy and the predischarge, helium pressure. In figure 10(a) the normal shock velocity that may be obtained in real air is shown as a function of the helium driver gas state and the initial driven air pressure. Figure 10(b) illustrates a practical range of operating conditions including the energy required in the capacitor bank to achieve these conditions. This assumes an overall efficiency of 50 percent which appears to be a reasonable estimate for initial helium pressure of 200 psi or above. Below an initial helium driver gas pressure of roughly 200 psi the efficiency decreases, although this depends on the magnitude of the discharge energy (ref. 6). The three initial driven air pressures used in figure 10(A) correspond to a range of altitudes where simulation of the normal shock speeds shown is of interest for manned flight (150 – 250,000 ft). To obtain a greater range of shock speeds for a given energy input, it is also possible to increase the range of initial driven pressures. The shock velocity and the initial driven air pressure (P_1) completely specify the normal shock parameters. Two of these parameters, the shock strength and the test gas velocity have been plotted, respectively, in figures 11 and 12 (refs. 3 and 4).

Variable area.- The design of a high performance shock tube for a specified range of operation must meet several economic, design, and operating constraints. If the measuring techniques and range of operation is fixed then the minimum driven chamber length and diameter are also fixed. Since the economic and design constraints are primarily concerned with the driver chamber there is a degree of flexibility, namely, a variable area shock tube.

Figure 1(b) illustrates that there is a minimum driver chamber length that will prevent the reflected expansion fan head from interfering with the test gas before the data is obtained. Figures 7 through 9 give the driver gas conditions as a function of the discharge energy per unit volume. Thus, to reduce the absolute value of the discharge energy, the volume of the driver chamber or the chamber diameter may be reduced below that of the driven chamber. This reduction of the driver chamber diameter is also an advantage in reducing the driver chamber strength requirements or wall thickness as shown in figure 13.

Figures 10(a) and 10(b) are performance charts for a constant area tube. It is desirable to investigate the performance characteristics of a variable area tube. This has been done (refs. 7 and 8) by considering

the effective driver gas properties. Figures 14 and 15 show, respectively, the effective driver gas temperature and pressure divided by the actual driver gas temperature and pressure in the reduced diameter driver chamber, as a function of the area ratio. The effective driver gas properties are denoted by a prime and are defined as the properties in a constant area shock tube that will achieve the same performance as the variable area tube. It is noted that both the effective temperature and the effective pressure decrease with increasing area ratio. Figures 14 and 15 may be used in conjunction with figure 10(A) to determine the performance characteristics for any area ratio.

If the driven chamber area is 15 times greater than that of the driver chamber, the total energy required to obtain a given shock velocity is roughly 15 percent of the energy required for the same shock tube with a constant area equal to the driven chamber area. This is for a helium-air shock tube and for velocities in excess of 25 kolofeet per second. Although this appears to be a considerable advantage from the standpoint of energy requirements, it is brought about only by a minimum diameter driven chamber requirement. This minimum diameter driven chamber requirement is due to viscous effects as discussed below. In fact, the shock velocity obtained for a given driver chamber, driver gas state, and driven gas pressure can be increased by decreasing the driven chamber diameter. For a high performance shock tube, however, the boundary layer effects become crucial.

Boundary layer effects.- There are extremely important practical restrictions to shock tube operation which stem from the viscous properties of real gases. At a given station in the driven chamber, the time for observing the test gas is limited to the time between the passing of the shock and the contact surface. If the initial formation of the shock wave is assumed to be instantaneous the test time may be expressed as,

$$\tau = \int_0^L \left(\frac{1}{U_s} - \frac{1}{U_{c.s.}} \right) dx \qquad (17)$$

at a distance L from the diaphragm. All of the previous relations and calculations are based on an inviscid flow which predicts that the shock velocity (U_s) and the contact surface velocity $(U_{c.s.})$ are constant. For these assumptions, where U_s and $U_{c.s.} = U_2$ are constant, an ideal test time may be obtained.

$$\left(\frac{\tau}{L} \right)_{ideal} = \frac{1}{U_s} - \frac{1}{U_2} \qquad (18)$$

This ideal test time per unit length has been plotted in figure 16 for various initial driven pressures. The data shown in this figure is considerably below the ideal case.

Although the inviscid assumption enables a fairly accurate prediction of the major flow in a shock tube, the actual flow contains a boundary layer which is initiated at the shock front. This boundary layer causes two interrelated effects. One is an attenuation or slowing down of the shock wave while the other is a depletion of the test gas by a mass flow from the test gas and into the boundary layer. The former effect reduces the performance of the shock tube flow below that which would be predicted by the inviscid analysis. The latter effect, however, can reduce the test time to the extent that it becomes impossible to obtain data by the use of stationary instrumentation.

Hooker (ref. 9) has evaluated the effects of the mass flux out of the test gas. The results may be thought of as two regimes of test time dependence on initial driven pressure. For high initial driven pressures, on the order of 1 mm Hg or above, the test time is on the order of 40 percent of the ideal test time. For lower pressures the test time decreases rapidly for decreasing pressure. Thus, to obtain sufficient test time requires a relatively high initial driven gas pressure. There are, of course, many additional factors which also influence the test time. For example, Anderson (ref. 10) has shown that the test time reaches a maximum and then decreases as it travels through the driven chamber. In addition, the adverse effect of low pressures on the test time is decreased with increasing driven chamber diameters. This is to be expected since the boundary layer area is roughly proportional to the diameter while the test gas flow is proportional to the diameter squared. In particular, this is a constraint which supports the variable area shock tube discussed in section 5.

The data in figure 16 serves to illustrate the order of magnitude obtained. The scatter is due to the differences between the facilities as well as a turbulent mixing at the contact surface. A plane contact surface, as shown in figure 1, would only result from a perfect diaphragm burst. It is possible for a poor, or uneven, diaphragm burst to induce enough turbulence at the contact surface for the available test time to be negligible.

Experimental capabilities.- The normal shock propagating into the driven section can be an excellent simulation of the normal shock produced at the stagnation point of an entry vehicle. In addition, the transient reaction of the driven gas as it passes through the normal shock and relaxes to chemical and thermodynamic equilibrium enables the study of chemical and reaction rates of the gas. It is noted that the radiation characteristics of a gas as it passes through a normal shock,

including the nonequilibrium and equilibrium radiation, may be obtained by effectively nonstationary instrumentation. For example, it is possible to have a photographic film moving at the same effective rate as the normal shock (ref. 11). This allows a continuous photograph of a shock as it propagates through a region of the driven chamber. The photograph may be in form of a spectrum of thermal radiation, limited only by the optical properties of the system (for example, lenses).

In many gas dynamic studies such as the determination of convective heat transfer rates, high temperature thermodynamic properties of gases, et cetera, it is desirable to use the shock tube to obtain extremely high stagnation conditions. These conditions are obtained by reflecting the shock wave either by the use of a model in the driven chamber or by the reflection at the downstream end of the driven chamber. The stagnation temperature, pressure, and enthalpy that may be obtained behind a reflected shock, are plotted, respectively, in figures 17 through 19 as a function of the shock velocity and the initial driven gas pressure. Figure 20 illustrates the shock velocity that is necessary to simulate the stagnation enthalpy encountered in flight for the flight velocity (U_∞) shown. The fact that the shock velocity is less than the simulated stagnation enthalpy flight velocity is obviously an advantage.

SHOCK TUNNELS

The shock tube is an extremely useful tool for the simulation and study of normal shocks and stagnation conditions. For the simulation and study of the hypersonic flow field about a body, however, the shock tunnel has definite advantages.

Principle of operation and analysis.- The main limitation to obtaining steady, high Mach number flow in a nozzle is that of obtaining sufficient stagnation conditions. The stagnation states obtained behind reflected shocks in the driven chamber of a shock tube (region 5 in figure 1(b)) cover a large range of conditions including high pressures and/or high enthalpies. The states that may be achieved in this region are illustrated in figures 17 through 19. A shock tunnel utilizes these stagnation conditions for the flow through a supersonic or hypersonic nozzle. The setup is illustrated schematically in figure 21.

Once the flow has been established, it is relatively steady for the duration of the stagnation conditions of state 5. If the shock tunnel flow is tailored (ref. 12), the flow time is limited either by the depletion of the test gas through the nozzle or more likely by the interaction of the reflected expansion fan head with the test gas. The tailored condition is obtained if the reflected shock wave does not interact with the contact surface. An interaction consists of a

secondary shock wave and expansion fan generated as the reflected shock wave passes through the contact surface.

During operation, the test gas of the shock tunnel is expanded from its stagnation state to a high velocity (U_6) and a low temperature and pressure. The expansion is nearly isentropic depending on the efficiency of the nozzle. As long as the pressure is sufficient, the test gas will remain in chemical and thermodynamic equilibrium as it expands. It is possible for the expanding test gas to become chemically frozen if the pressure is too low. This effect has not been considered in this report but may be considered as detrimental.

In general, the area of the throat in a hypersonic shock tunnel is negligible as compared to the area of the shock tube driven chamber. Thus, the reflection of the normal shock wave was considered to be complete. In addition, any decrease in the stagnation enthalpy due to heat transfer and thermal radiation has been neglected. The expansion of the test gas through the hypersonic nozzle has been assumed to be isentropic.

Performance characteristics.- The performance range of a hypersonic shock tunnel is illustrated in figure 22. This figure illustrates the combinations of Reynolds number per foot and Mach number that may be achieved by the expanded test gas. The maximum stagnation pressure has been selected as 3,000 Atm. based on the results of figure 13. The range of operation may be extended by varying this pressure as shown in figure 22 where a stagnation pressure of 100 Atm. has also been considered. The liquification limit is drawn as the point at which the air begins to liquify based on a 3,000 Atm. stagnation pressure. An increase in the stagnation pressure will increase the Reynolds number that may be obtained before liquification. The low enthalpy limit $\left(\frac{h}{RT_o} = 20\right)$ is established by the capabilities of the shock tube and the relatively low Mach numbers that may be obtained. The high enthalpy limit $\left(\frac{h}{RT_o} = 400\right)$ is established by the convective heating and erosion problems at the nozzle throat as well as the thermal radiation losses from the stagnation test gas. The area ratio limit $\left(\frac{A_6}{A^x} = 10^6\right)$ is relatively arbitrary; however, the low pressures ($\sim 10^{-5}$ Atm.) and large nozzles required at this limit result in a reasonable restriction.

The time limitation of steady flow for the range of conditions shown in figure 22 is established by nozzle throat heating problems and by the duration of the stagnation conditions. The testing time for a shock tunnel is on the order of milliseconds as opposed to the microsecond range of a shock tube.

Driver mechanism.- In principle, a shock tunnel may be driven by many mechanisms, including pressure driven, combustion driven, and electrically charged shock tubes. However, the tailored operation of a shock tunnel requires the same pressure and density ratio across the reflected shock in both the test gas and the expanded driver gas (ref. 12). This requires a certain γ_3 and T_3 depending on the driver gas and the driven gas. To obtain a range of reflected and tailored conditions, a range of γ_3 and T_3 combinations is required. This may be accomplished by using a range of driver stagnation conditions in various mixtures of driver gases. The electric arc discharge is probably the most versatile driver mechanism since there is no limit on the driver gas or gases that may be used and the range of driver gas stagnation conditions is greatest. In addition, the electric arc discharge process has a high degree of repeatability.

Experimental capabilities.- The Mach number, Reynolds number range of a hypersonic shock tunnel is considerable. It is extremely useful for flow field studies including heat transfer and pressure distributions as well as basic studies concerning nozzle flow and expanding gases.

It is to be noted, however, that although certain flight parameters may be simulated, complete simulation is in general not possible. For example, the high Mach number range shown in figure 22 is accomplished by extremely low free stream temperatures and not necessarily by high velocities. In addition, the real gas effects of air do not scale from the model used in a shock tunnel to the full-scale vehicle unless the phenomena are completely understood.

CONCLUDING REMARKS

The characteristics of an electrically charged helium driver gas shock tube and of a shock tunnel have been outlined above. The specific capabilities of these facilities permit the experimental study of many aspects of manned vehicle entry heating problems.

REFERENCES

1. Wright, J. K.: Shock Tubes. New York, John Wiley and Sons, Inc., 1961.

2. Glass, I. I., and Patterson, G. N.: A Theoretical and Experimental Study of Shock-Tube Flow. J. Aeronautical Sci., vol. 22, 73, 1955.

3. Trimpi, Robert L.: A Preliminary Theoretical Study of the Expansion Tube, A New Device for Producing High-Enthalpy Short-Duration Hypersonic Gas Flows, NASA TR R-133, 1962.

4. Feldman, Saul: Hypersonic Gas Dynamic Charts for Equilibrium Air. Res. Rep. 40, Avco Res. Lab., January 1957.

5. Ziemer, Richard W.: Extended Hypervelocity Gas Dynamic Charts for Equilibrium Air. STL/TR-60-0000-09093, Space Technology Laboratories, Inc., April 14, 1960.

6. Warren, W. R., Rogers, D. A., and Harris, C. J.: The Development of an Electrically Heated Shock Diver Test Facility. Second Symposium on Hypervelocity Techniques, University of Denver, Denver, Colorado, March 20, 1962.

7. Lin, Shao-In, and Fyfe, Walter I.: Low-Density Shock Tube for Chemical Kinetic Studies. Avco Research Laboratory Res. Rep. 91, July 1960.

8. Camm, John C.: Escape-Velocity Shock Tube With Arc-Heated Driver, Avco Research Laboratory, Second National Symposium on Hypervelocity Techniques, University of Denver, Denver, Colorado, March 20, 1962.

9. Hooker, William J.: Testing Time and Contact-Zone Phenomena in Shock-Tube Flows. Physics of Fluids, vol. 4, no. 12, 1451, December 1961.

10. Anderson, G. F.: Shock Tube Testing Time. J. Aerospace Sci., vol. 26, no. 3, 184, March 1959.

11. Allen, R. A., Camm, J. C., and Keck, J. C.: Radiation from Hot Nitrogen. Avco Research Lab Res. Rep. 102, April 1961.

12. Wittliff, Charles E., Wilson, Merle R., and Hertzberg, Abraham: The Tailored-Interface Hypersonic Shock Tunnel. J. Aerospace Sci., vol. 26, no. 4, 219, April 1959.

13. Shapiro, Ascher H.: The Dynamics and Thermodynamics of Compressible Fluid Flow, vol. I, II, New York. The Ronald Press Co., 1953.

14. Moeckel, W. E., and Weston, Kenneth C.: Composition and Thermodynamic Properties of Air in Chemical Equilibrium. NACA TN-4265, 1958.

15. Hanse, C. Frederick: Approximations for the Thermodynamic and Transport Properties of High Temperature Air. NASA TR R-50, 1959.

16. Ames Research Staff: Equations, Tables, and Charts for Compressible Flow. NACA Report 1135, 1953.

17. Trimpi, Robert L., and Cohen, Nathaniel B.: A Non-Linear Theory for Predicting the Effects of Unsteady Laminar, Turbulent of Transitional Boundary Layers on the Attenuation of Shock Waves in a Shock Tube with Experimental Comparison. NASA TR R-85, 1961.

18. Rose, P. H., and Stark, W. I.: Stagnation Point Heat Transfer Measurements in Dissociated Air. Avco Research Lab. Res. Rep. 3, April 1957.

19. Rose, P. H., and Riddell, F. R.: An Investigation of Stagnation Point Heat Transfer in Dissociated Air. Avco Research Lab. Res. Rep. 7, April 1957.

20. Henshall, Brian D., Teng, Robert N., and Wood, Albert D.: Development of Very High Enthalpy Shock Tunnels With Extended Steady-State Test Times. Research and Advanced Development Division, Avco Corp., Tech. Rep. RAD-TR-62-16, April 15, 1962.

21. Bloxsom, D. E., Jr.: Use of Capacitor Discharges to Produce High Temperature, High Pressure Air. Jet Propulsion, Sept. 1958.

22. Kantrowitz, Arthur: The Formation and Stability of Normal Shock Waves in Channel Flows. NACA TN-1225, March 1947.

23. Offenhartz, E., Weisblatt, H., and Flagg, R. F.: Stagnation Point Heat Transfer Measurements at Super-Satellite Speeds, J. Royal Aeronautical Society, January 1962.

24. Offenhartz, E., and Weisblatt, H.: Determination of the Time History of the Flow Field About Various Blunt Body Shapes and Sizes During Experiments in 1.5 Inches Diameter Shock Tube. Research and Advanced Development Division, Avco Corp., RAD-TR-2-58-10, July 15, 1958.

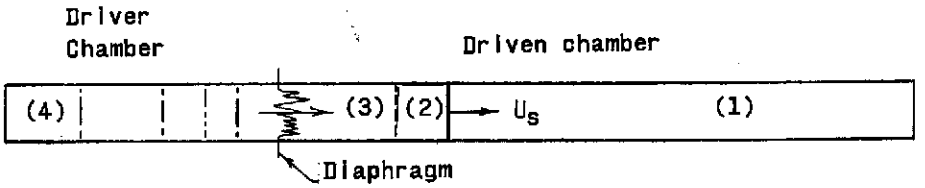

Figure 1a.- Shocktube at time θ shown below.

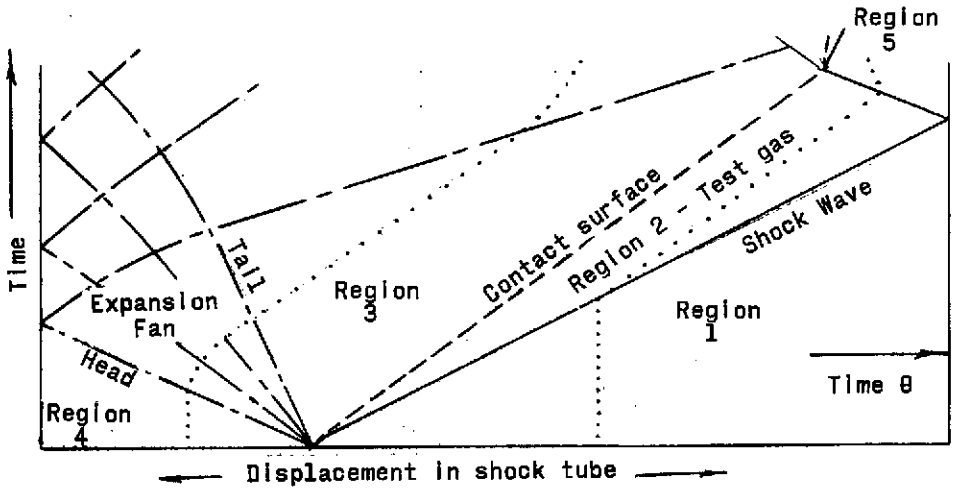

Figure 1b.- Shock tube, time - displacement diagram.

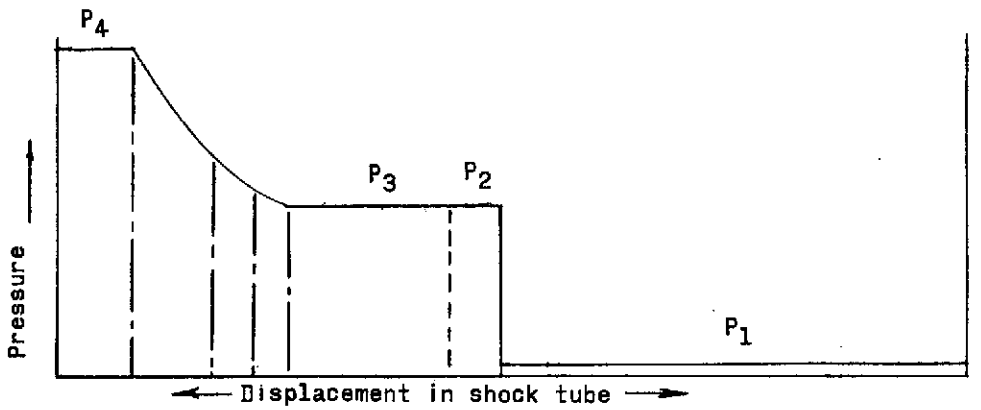

Figure 1c.- Pressure - displacement at time θ shown above.

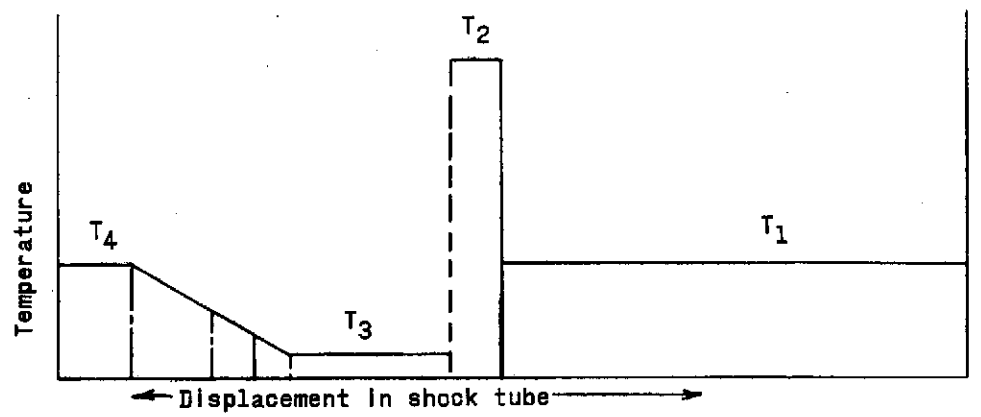

Figure 1d.- Temperature - displacement at time θ shown above.

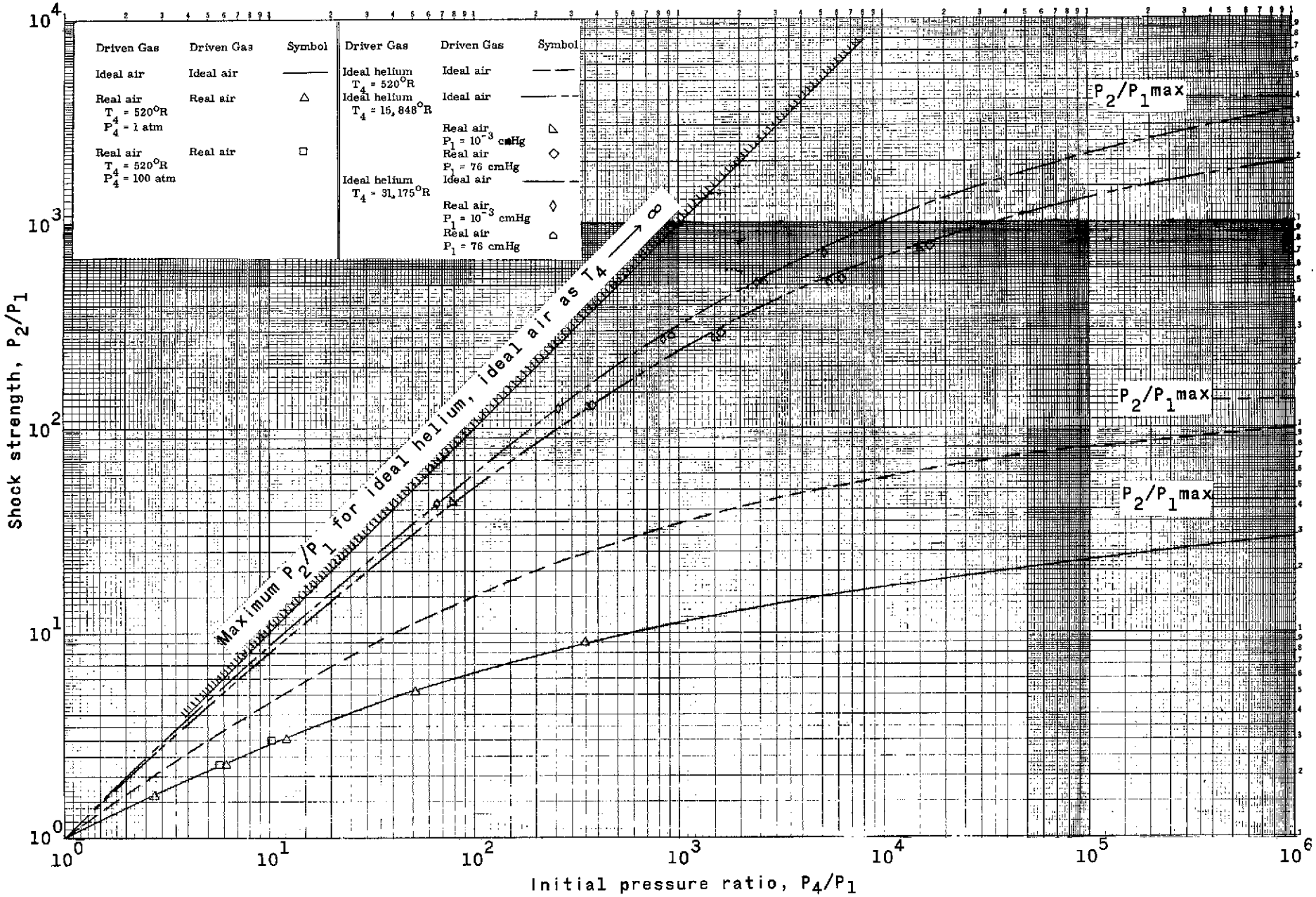

Figure 2.- Shock strength vs initial pressure ratio.

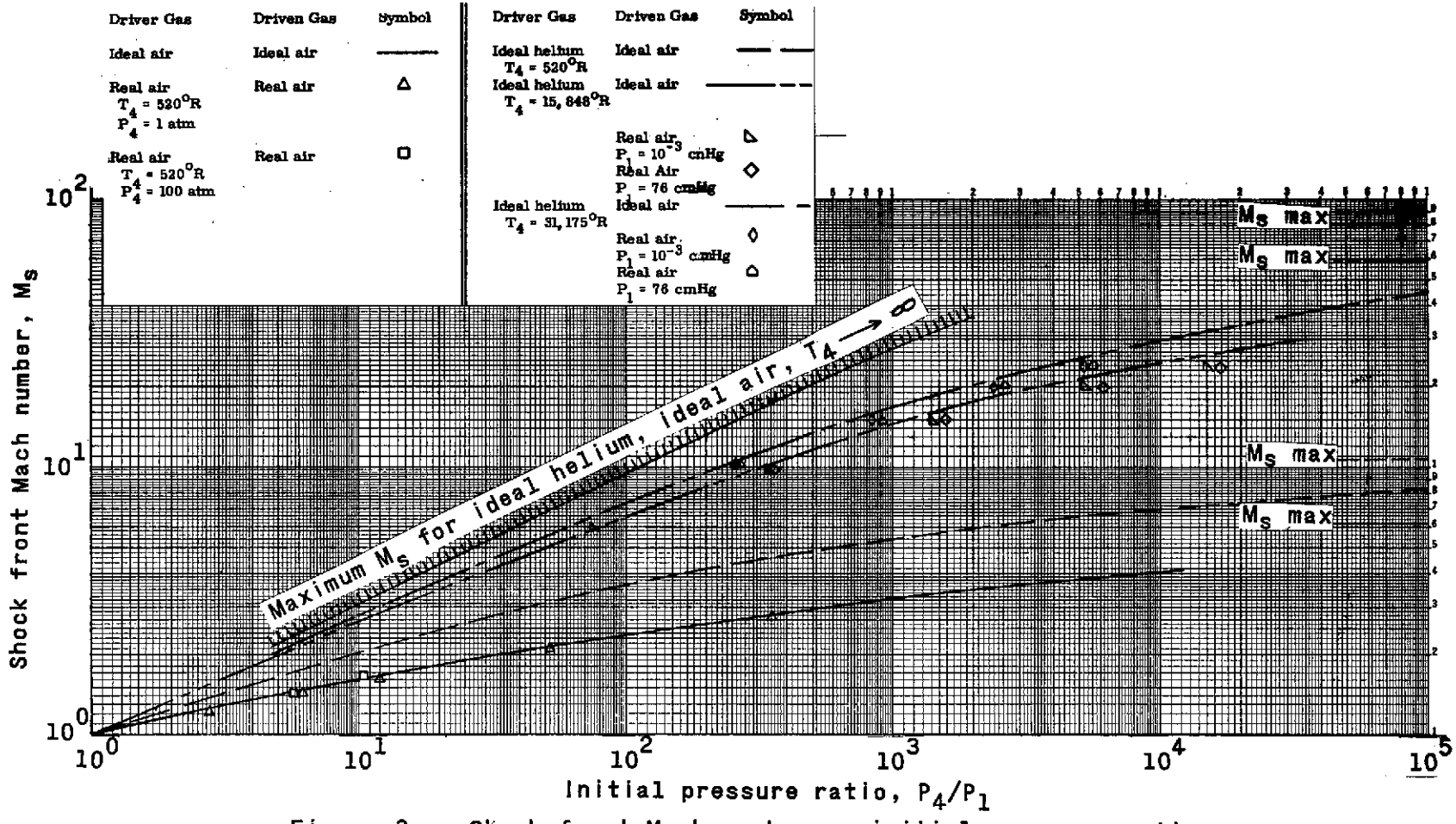

Figure 3.- Shock front Mach number vs initial pressure ratio.

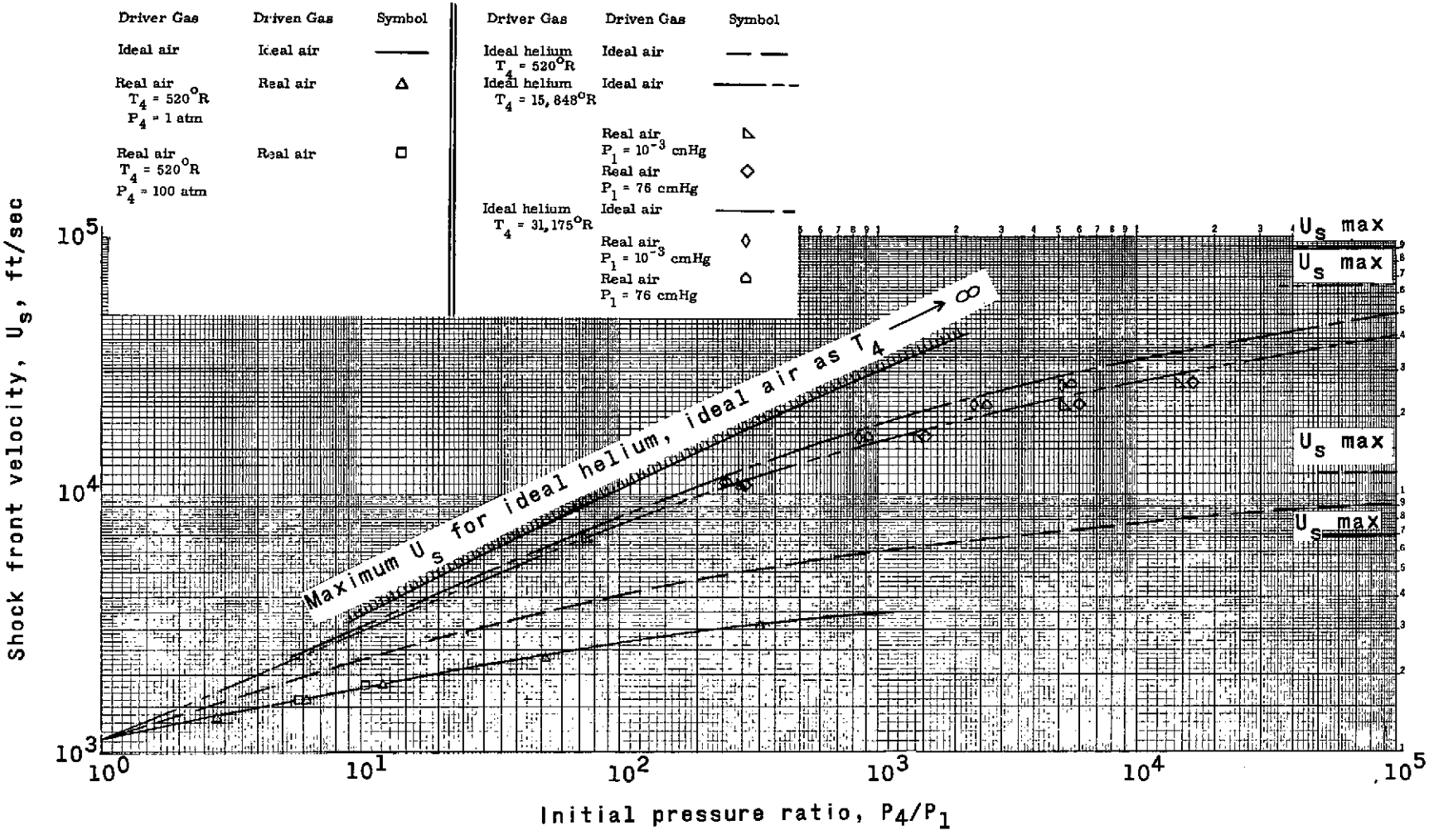

Figure 4.- Shock front velocity vs initial pressure ratio.

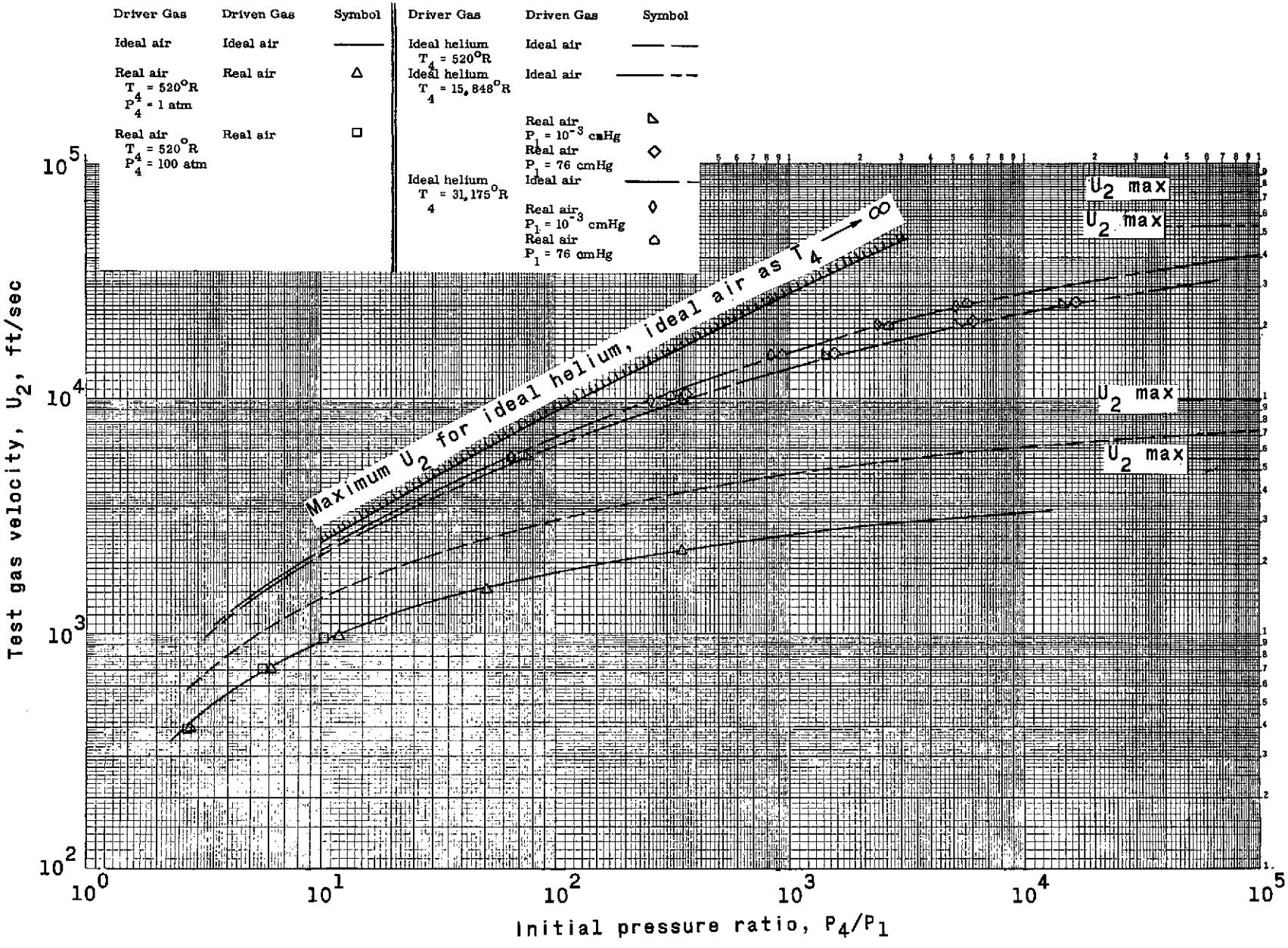

Figure 5.- Test gas velocity vs initial pressure ratio.

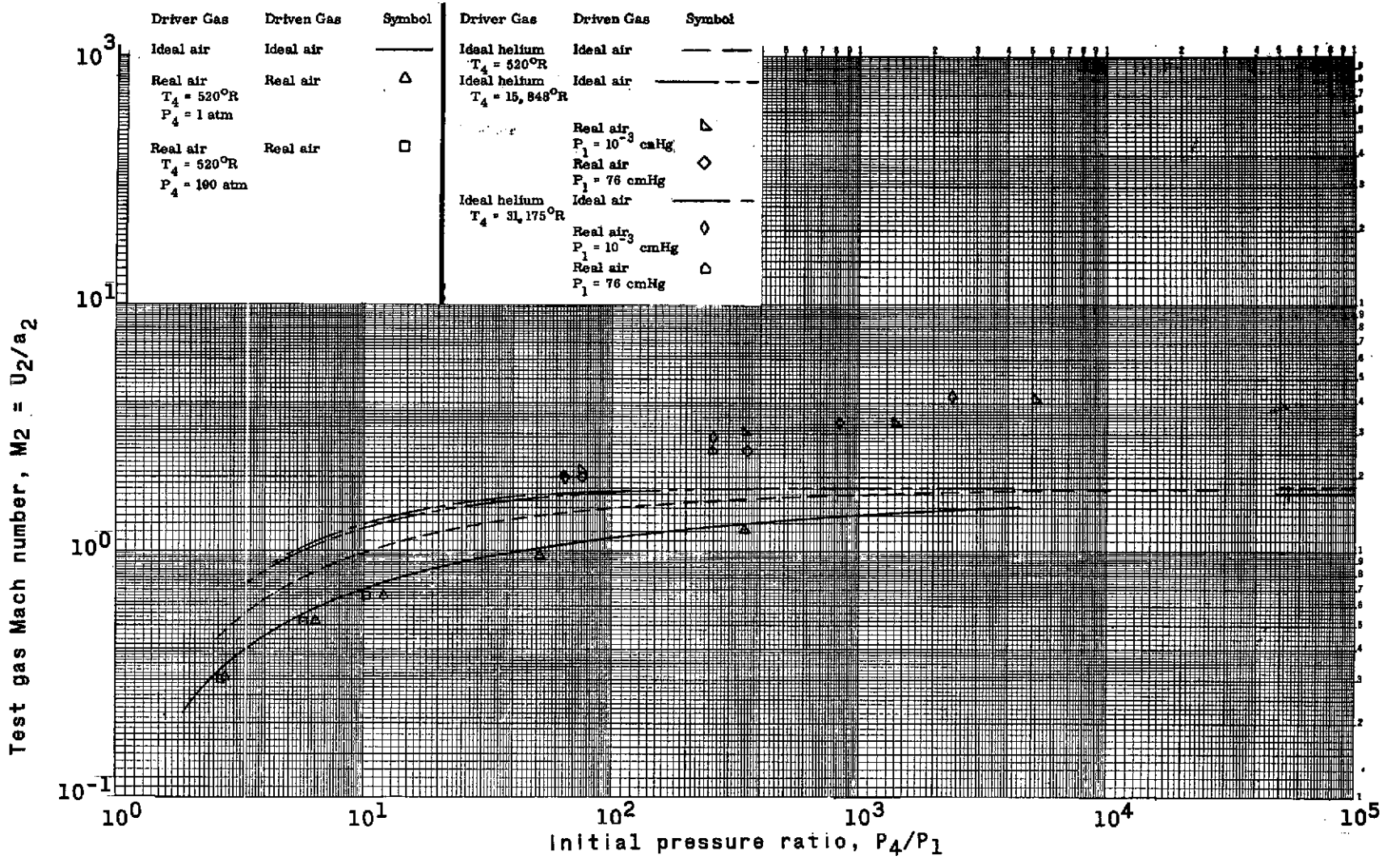

Figure 6.- Test gas Mach number vs initial pressure ratio.

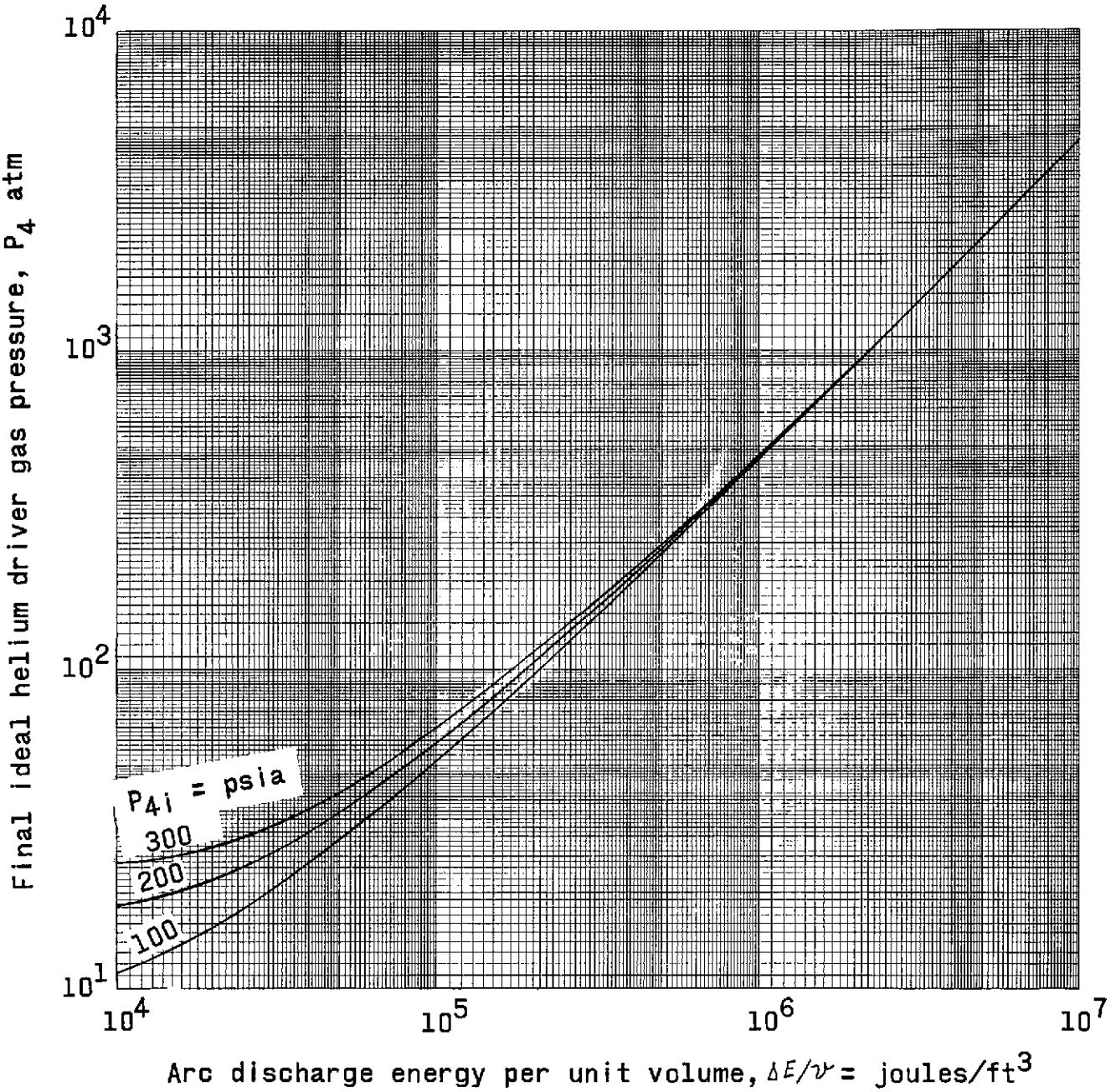

Figure 7.- The final ideal helium driver gas pressure as a function of the arc discharge energy per unit volume of driver gas.

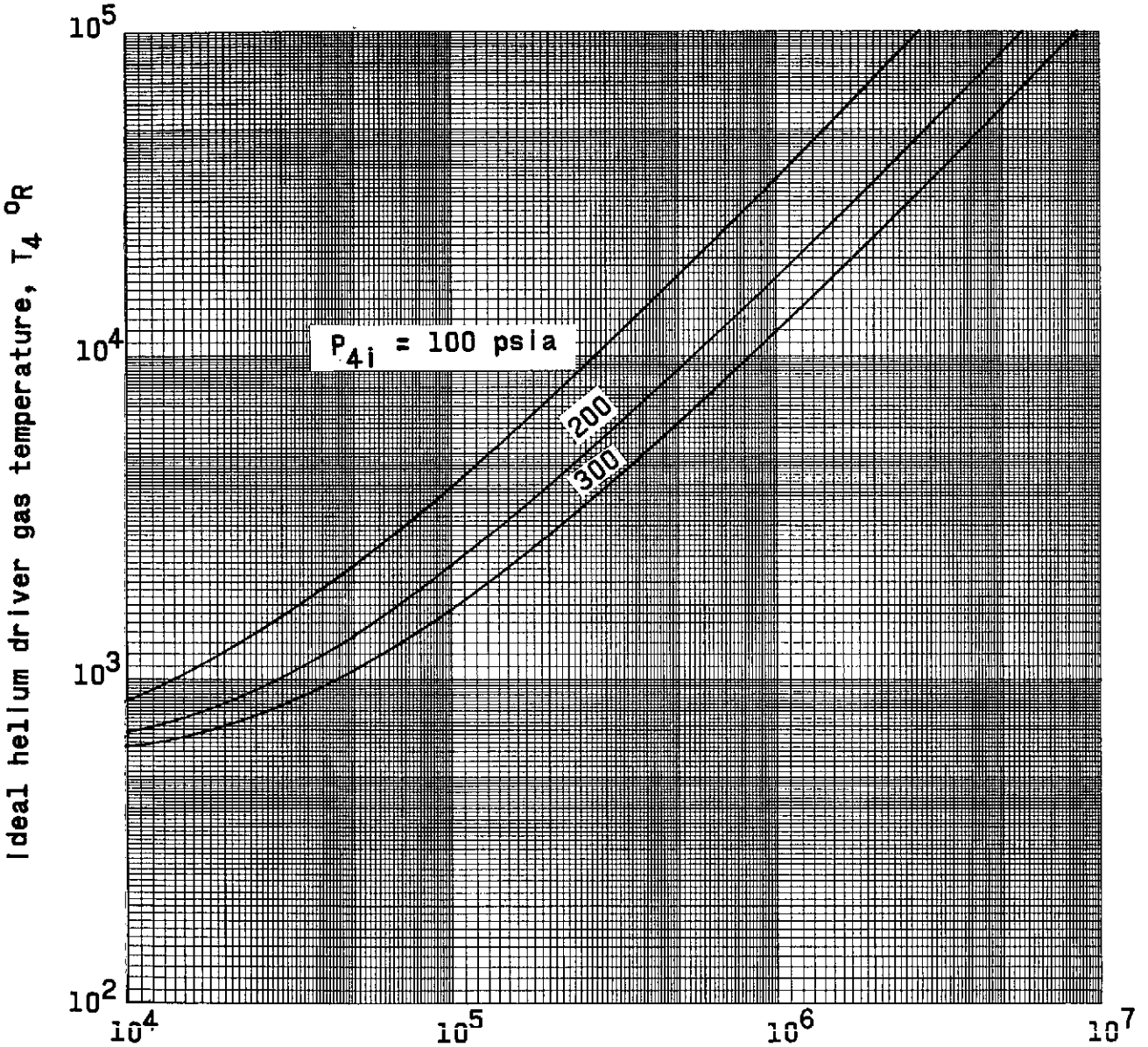

Figure 8.- The final ideal helium driver gas temperature as a function of the arc discharge energy per unit volume of driver gas.

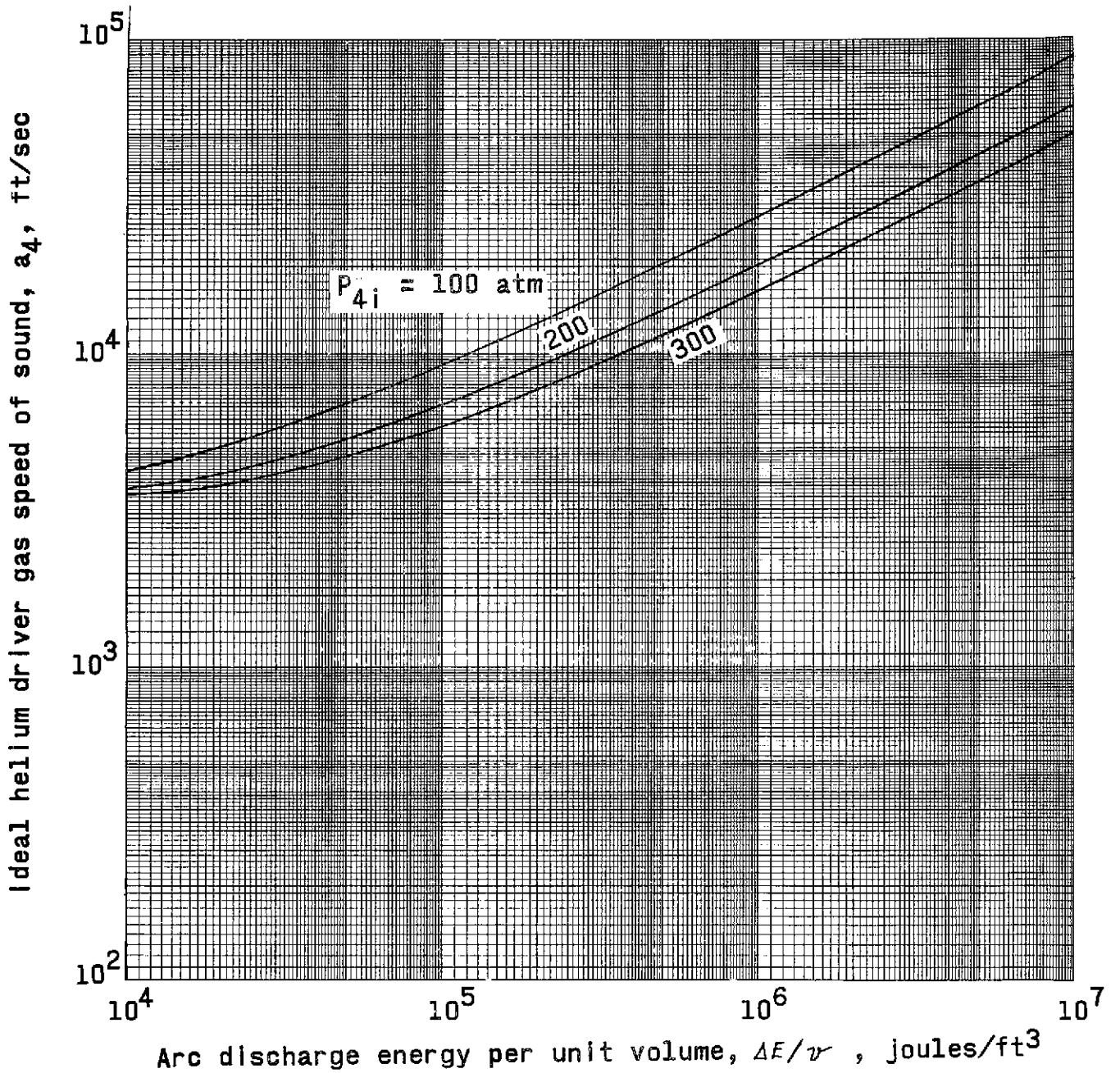

Figure 9.- Final ideal helium driver gas speed of sound as a function of the arc discharge energy per unit volume of driver gas.

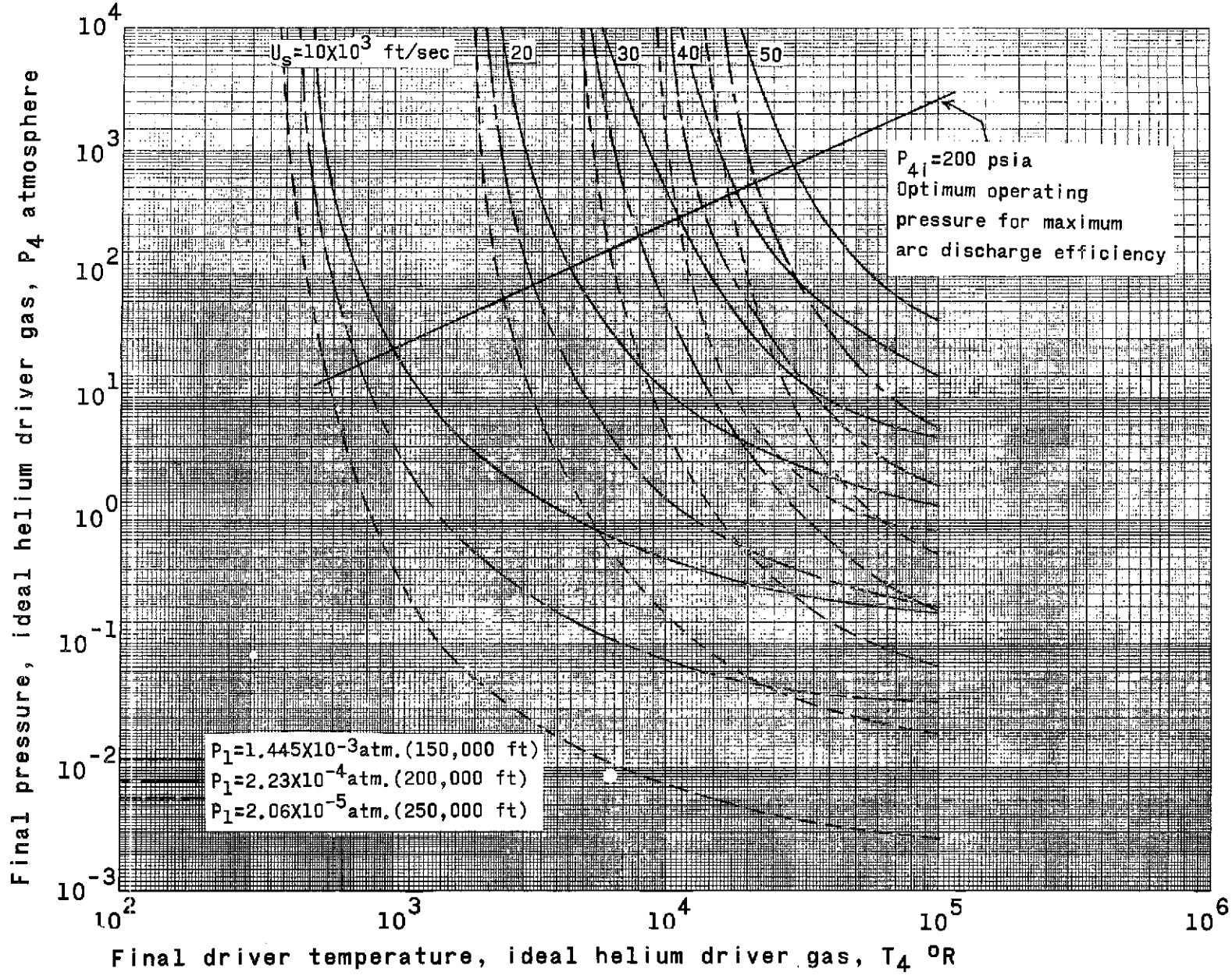

Figure 10a.- Shock velocity obtained in a constant area shock tube with real air driven gas as a function of the ideal helium driver gas state.

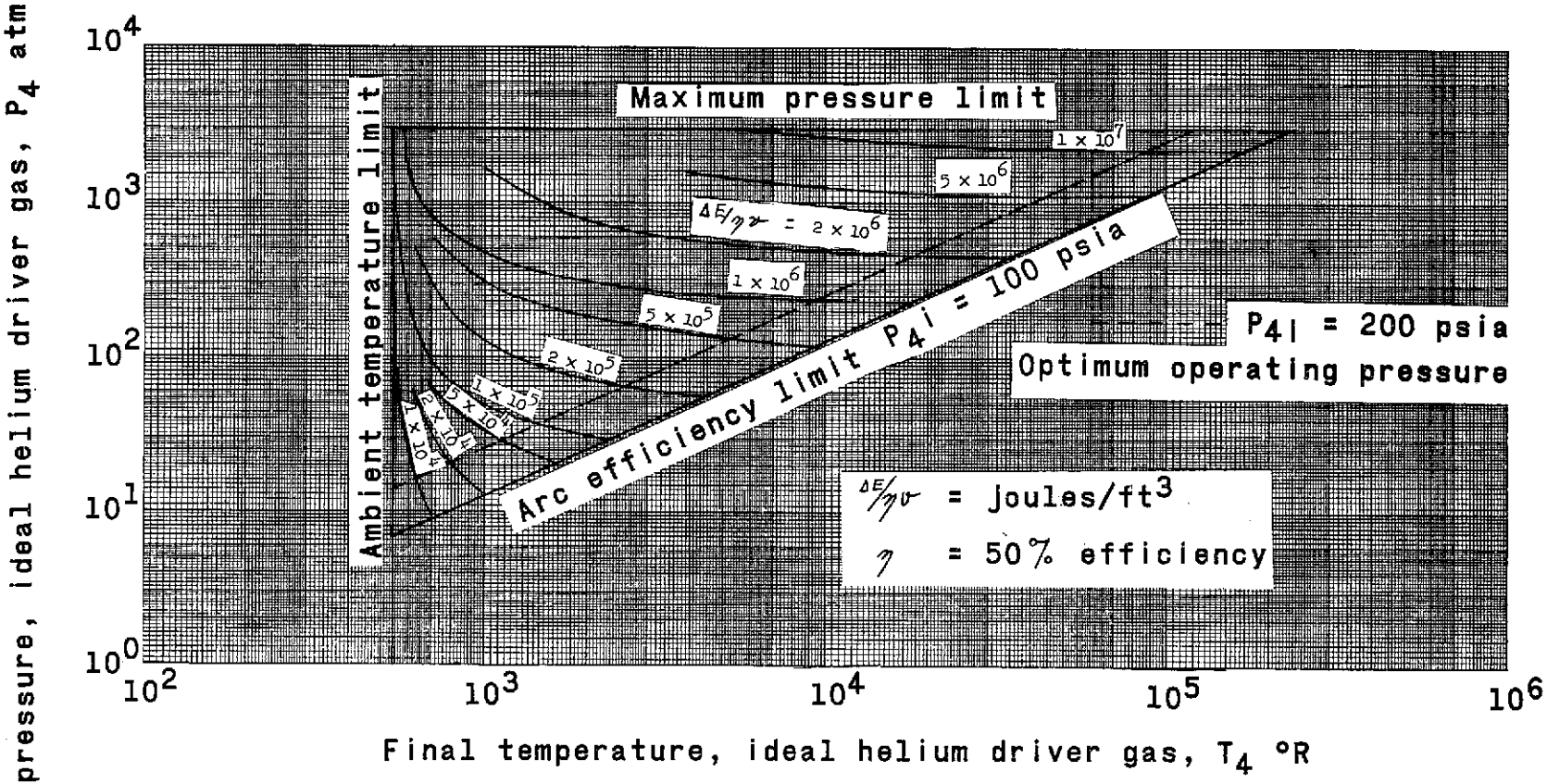

Figure 10b.- Operating range for an electrically charged, ideal helium driver.

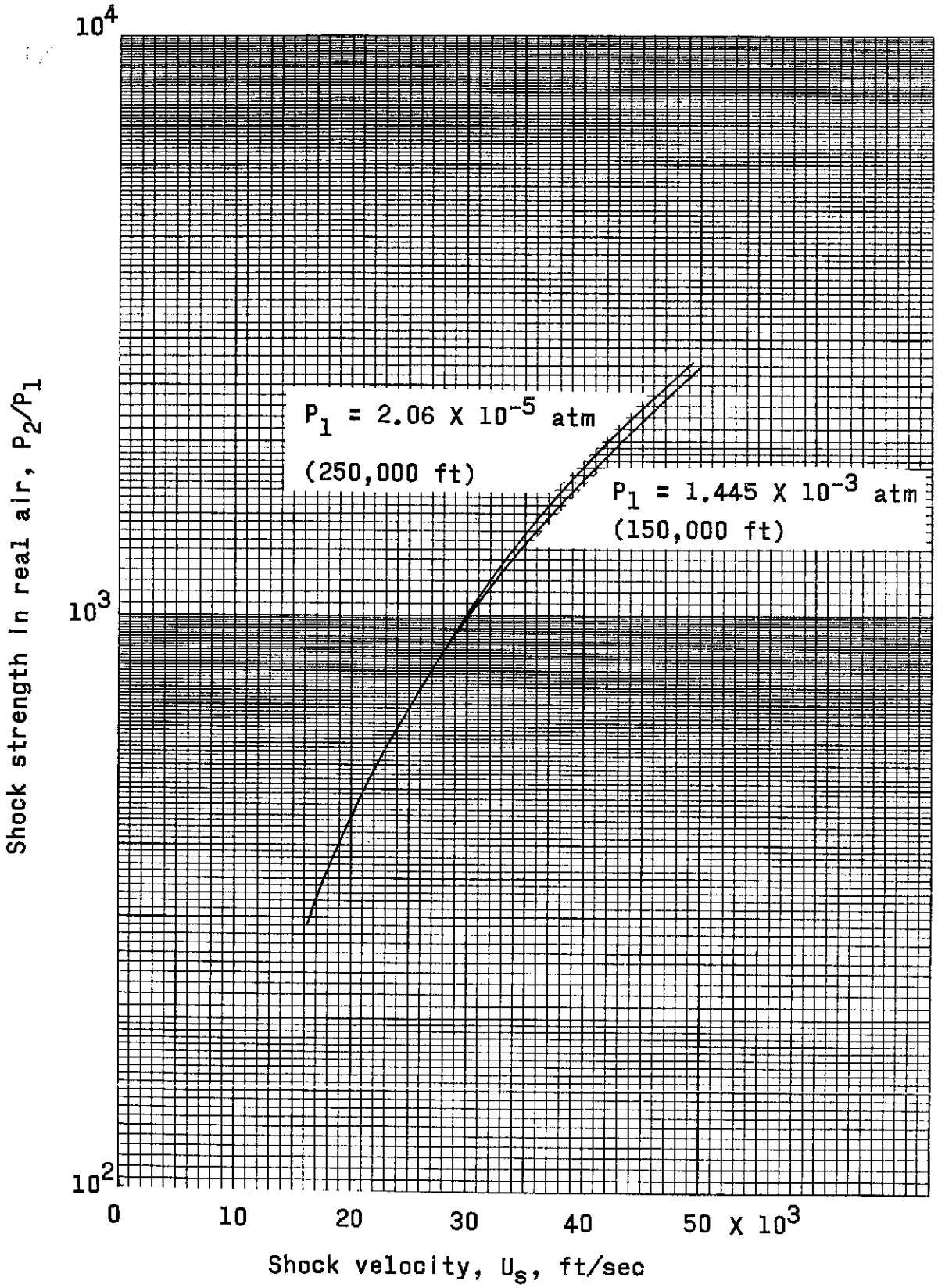

Figure 11.- Shock strength in real air vs normal shock velocity.

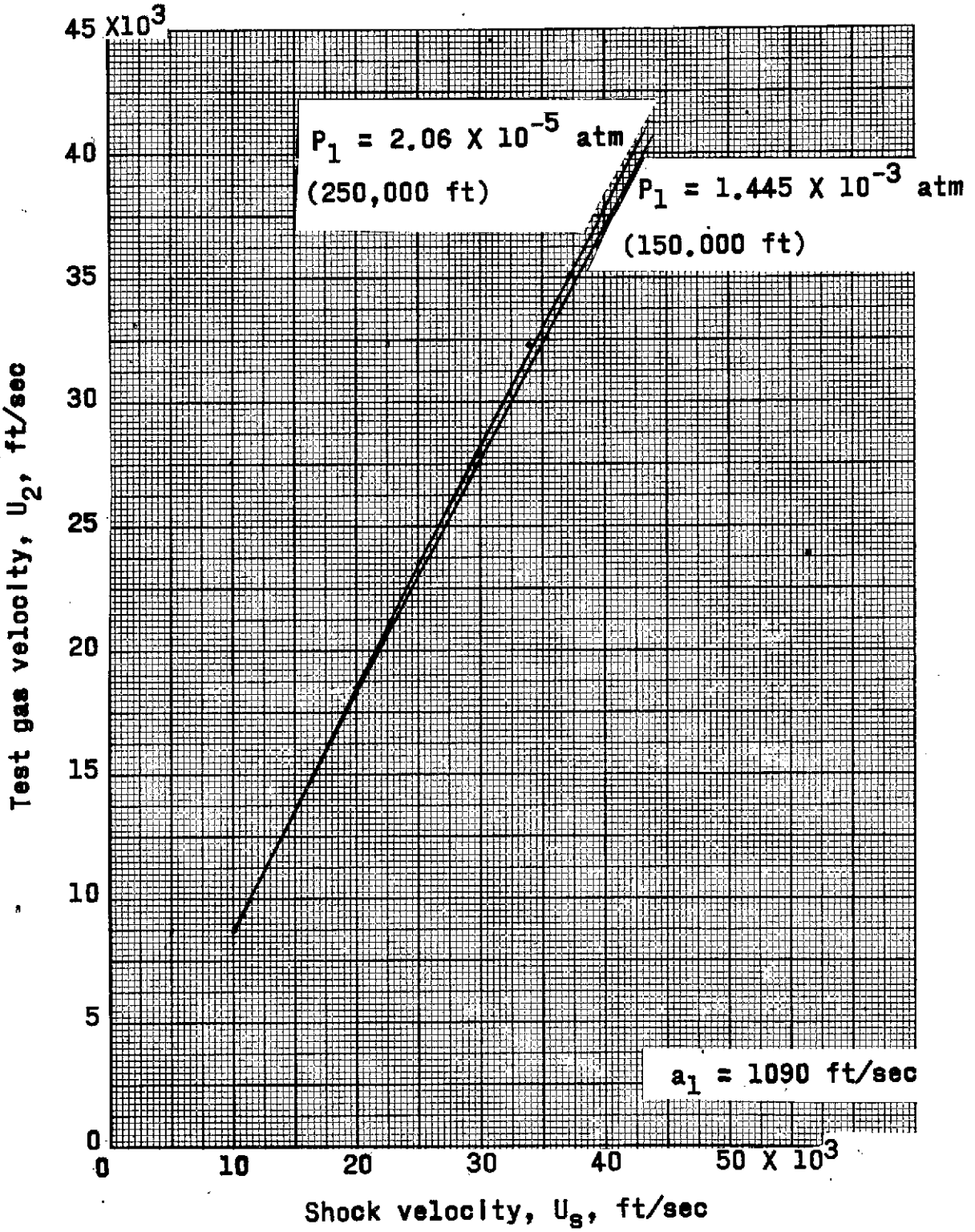

Figure 12.- Test gas velocity vs shock velocity in real air.

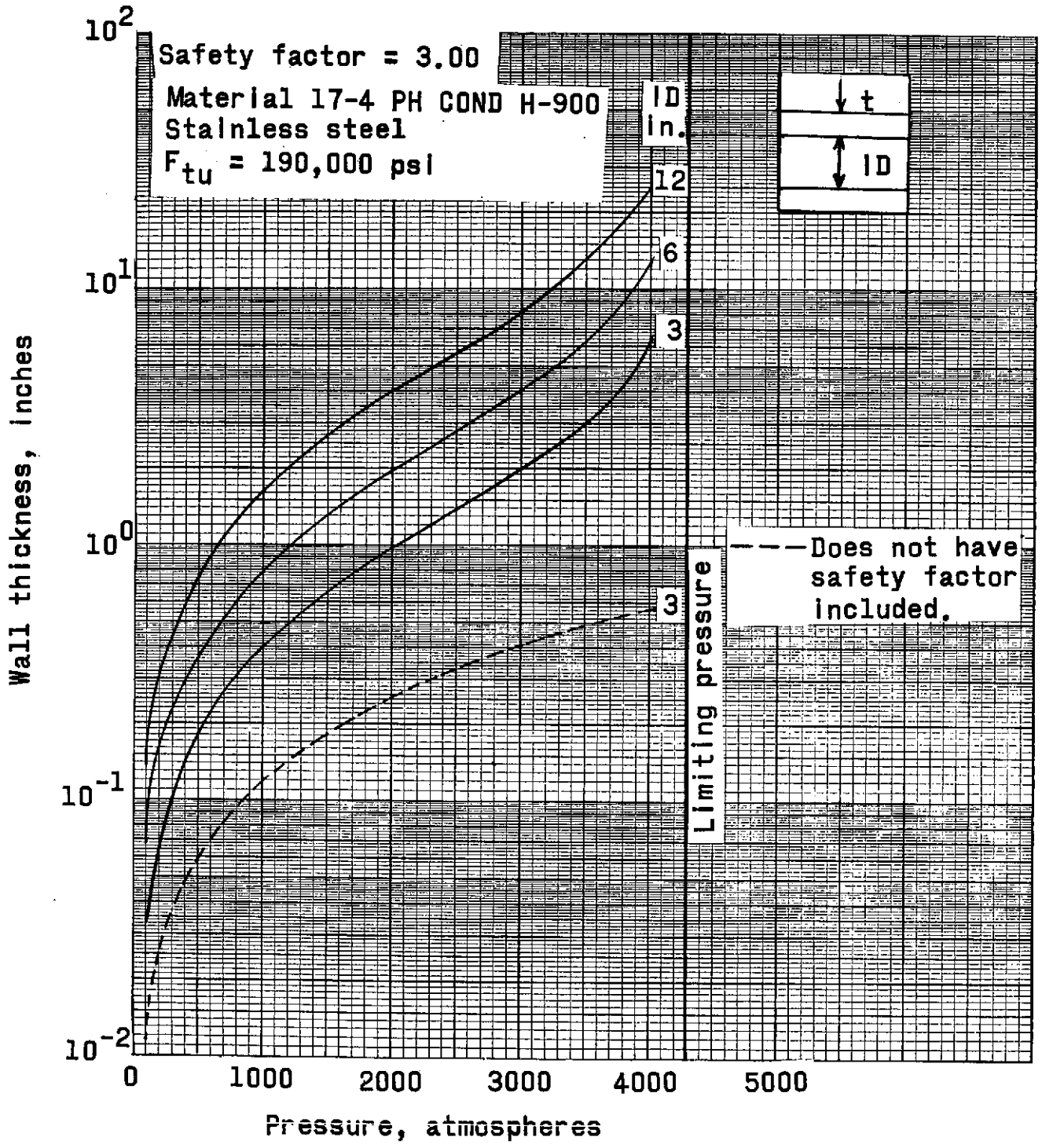

Figure 13.- Driver chamber size requirements as a function of static pressure.

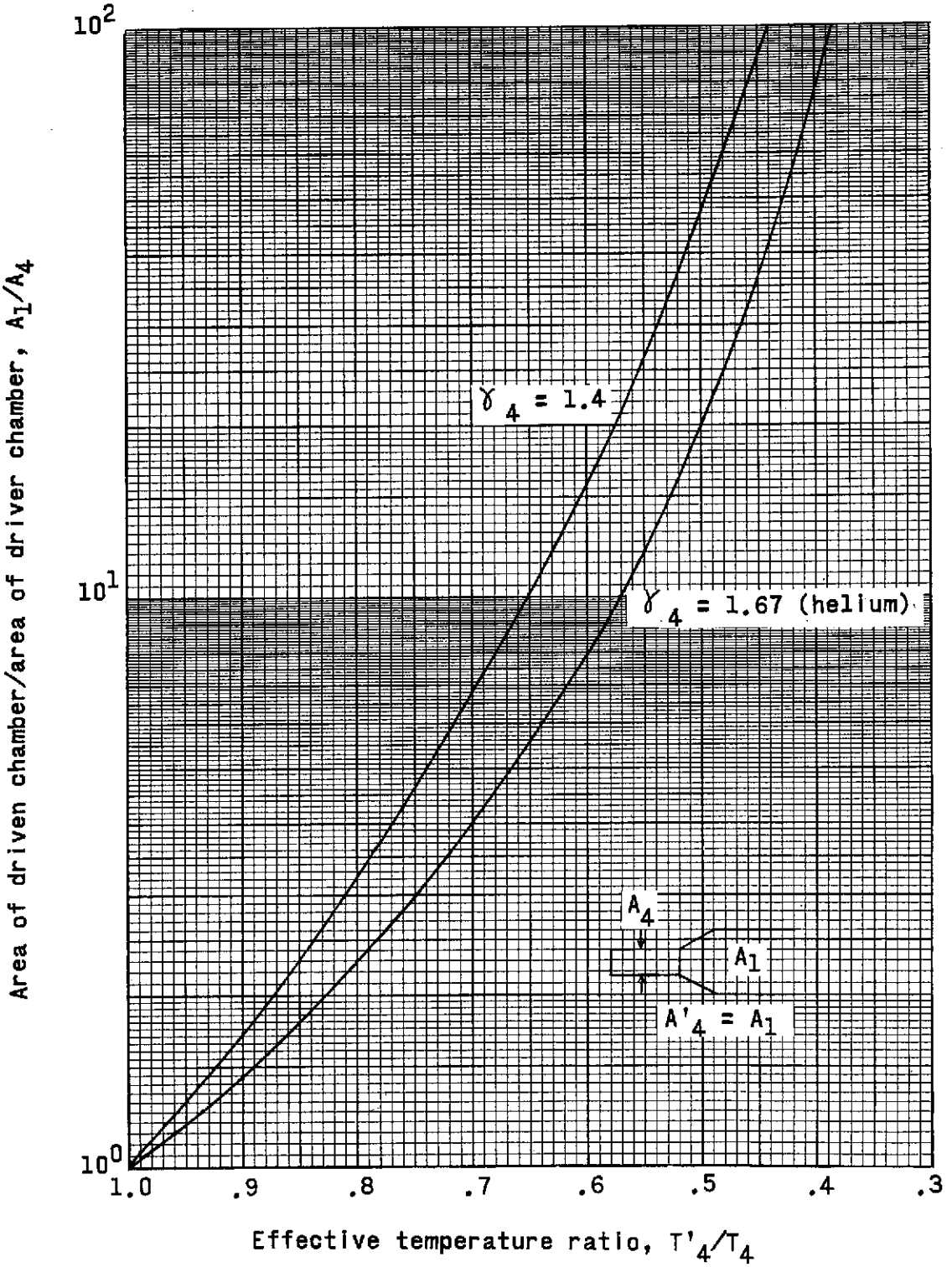

Figure 14.- Effective driver gas temperature based on a constant area shock tube divided by the actual driver gas temperature vs area ratio of shock tube.

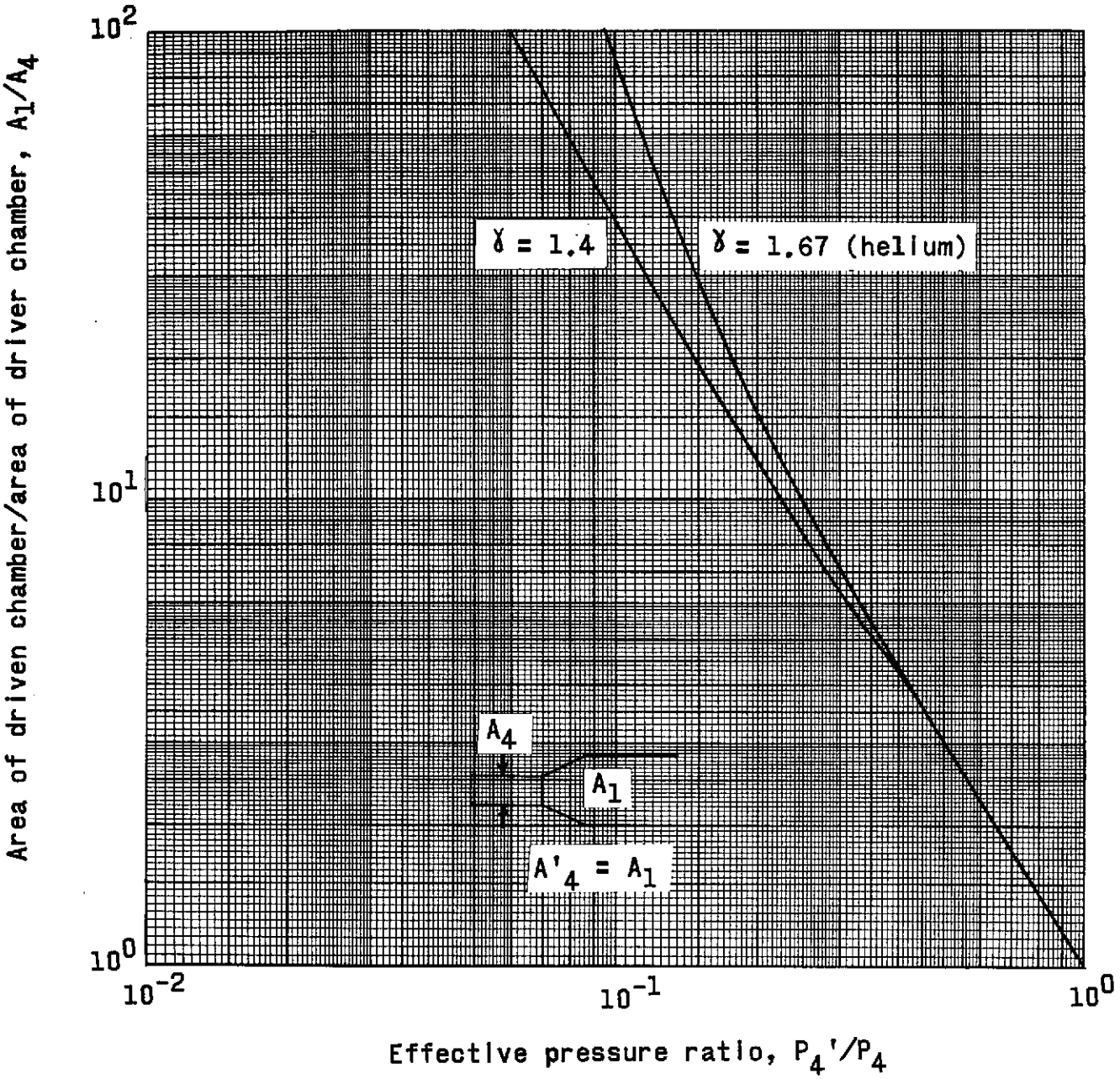

Figure 15.- Effective driver gas pressure based on a constant area shock tube divided by the actual driver gas pressure vs area ratio of shock tube.

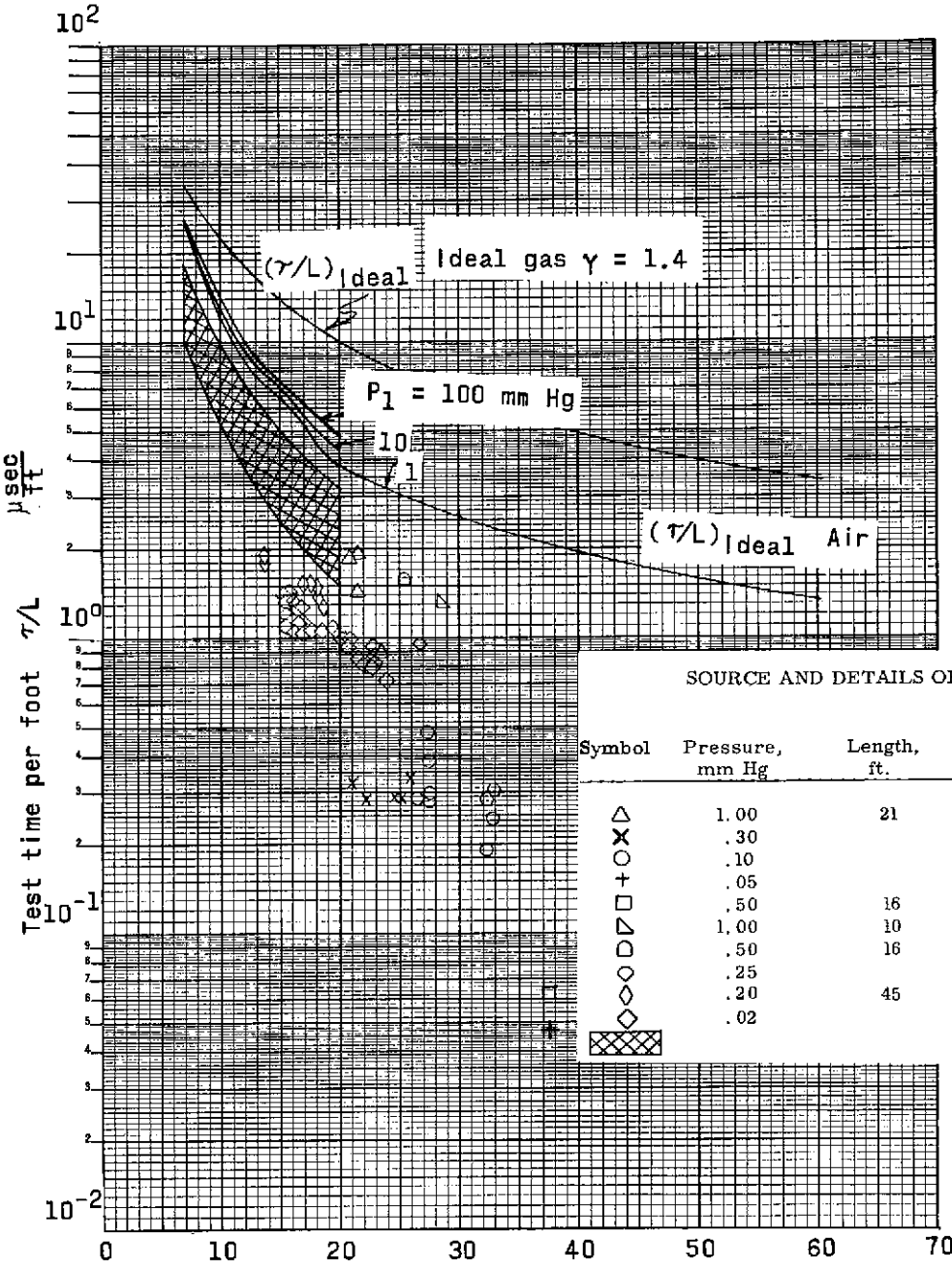

SOURCE AND DETAILS OF DATA POINTS

Symbol	Pressure, mm Hg	Length, ft.	Diameter, in.	Reference
△	1.00	21	6.0	7
X	.30			
○	.10			
+	.05			
□	.50	16	1.5	
▷	1.00	10	2.0	5
▯	.50	16	1.5	23
⬭	.25			
◇	.20	45	24.0	6
◇	.02			
▨			1.5	18

Figure 16.- Test time per foot versus shock velocity.

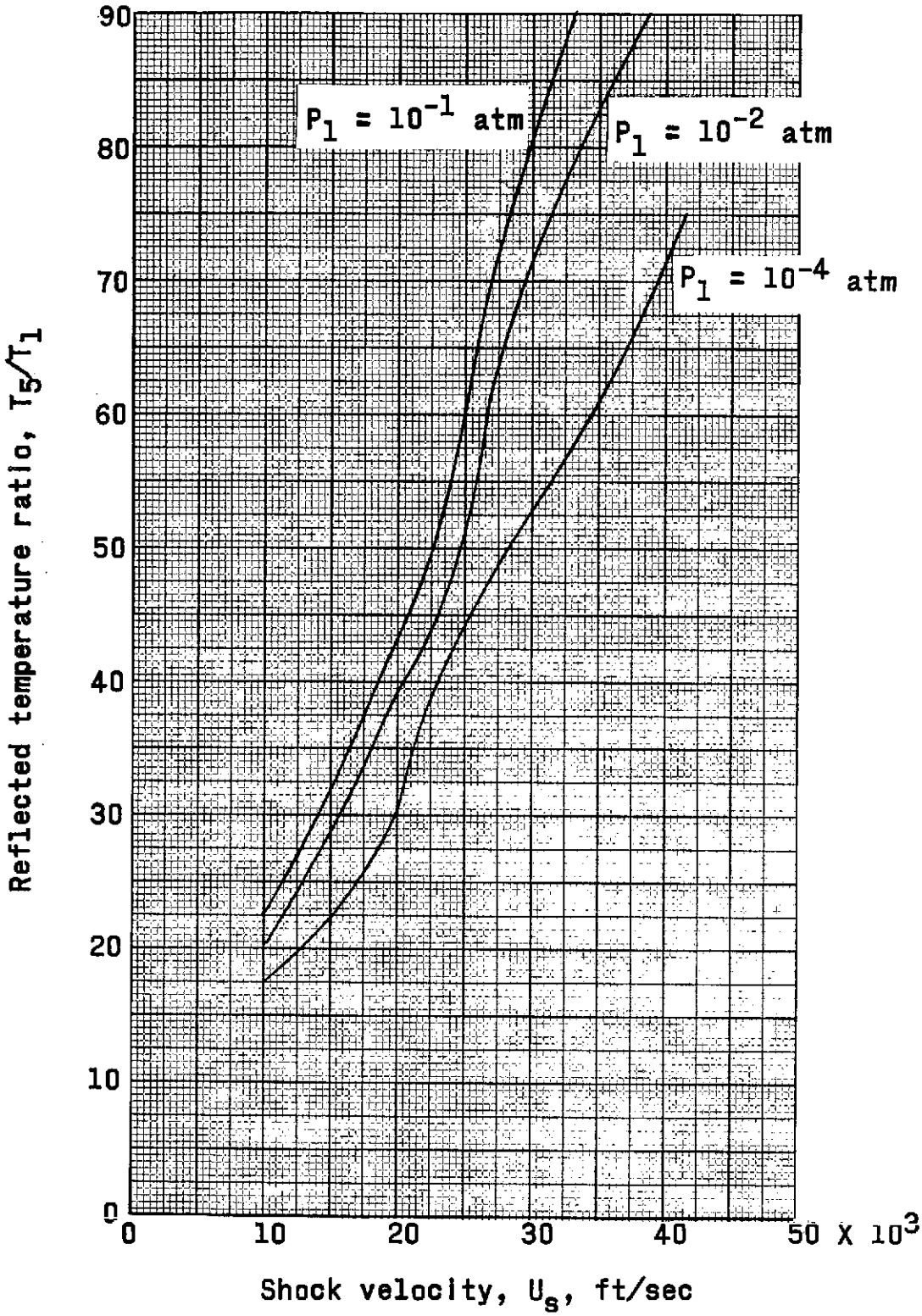

Figure 17.- Reflected shock temperature divided by initial driven air temperature vs shock velocity.

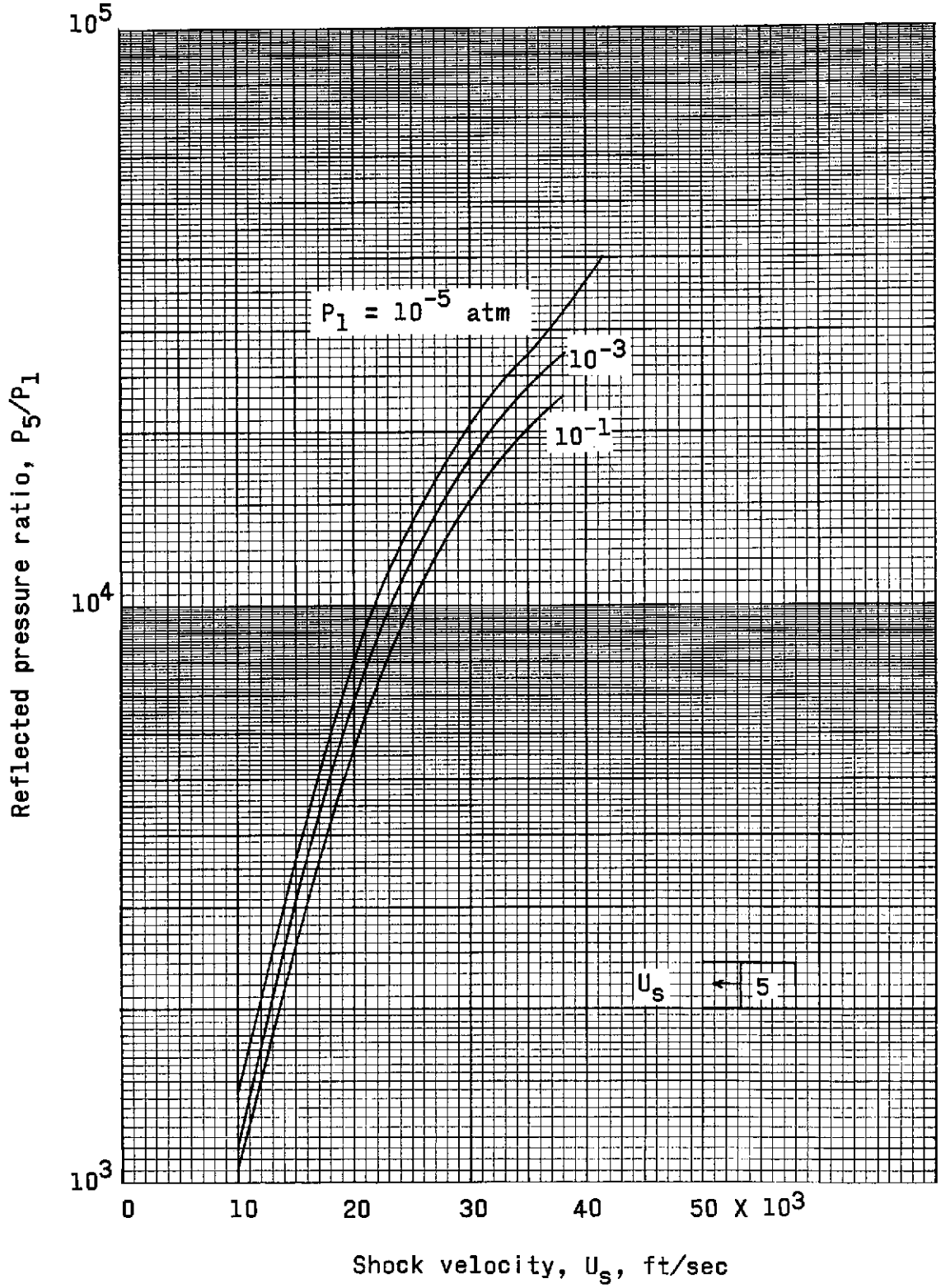

Figure 18.- Reflected shock pressure divided by initial driven air pressure vs shock velocity.

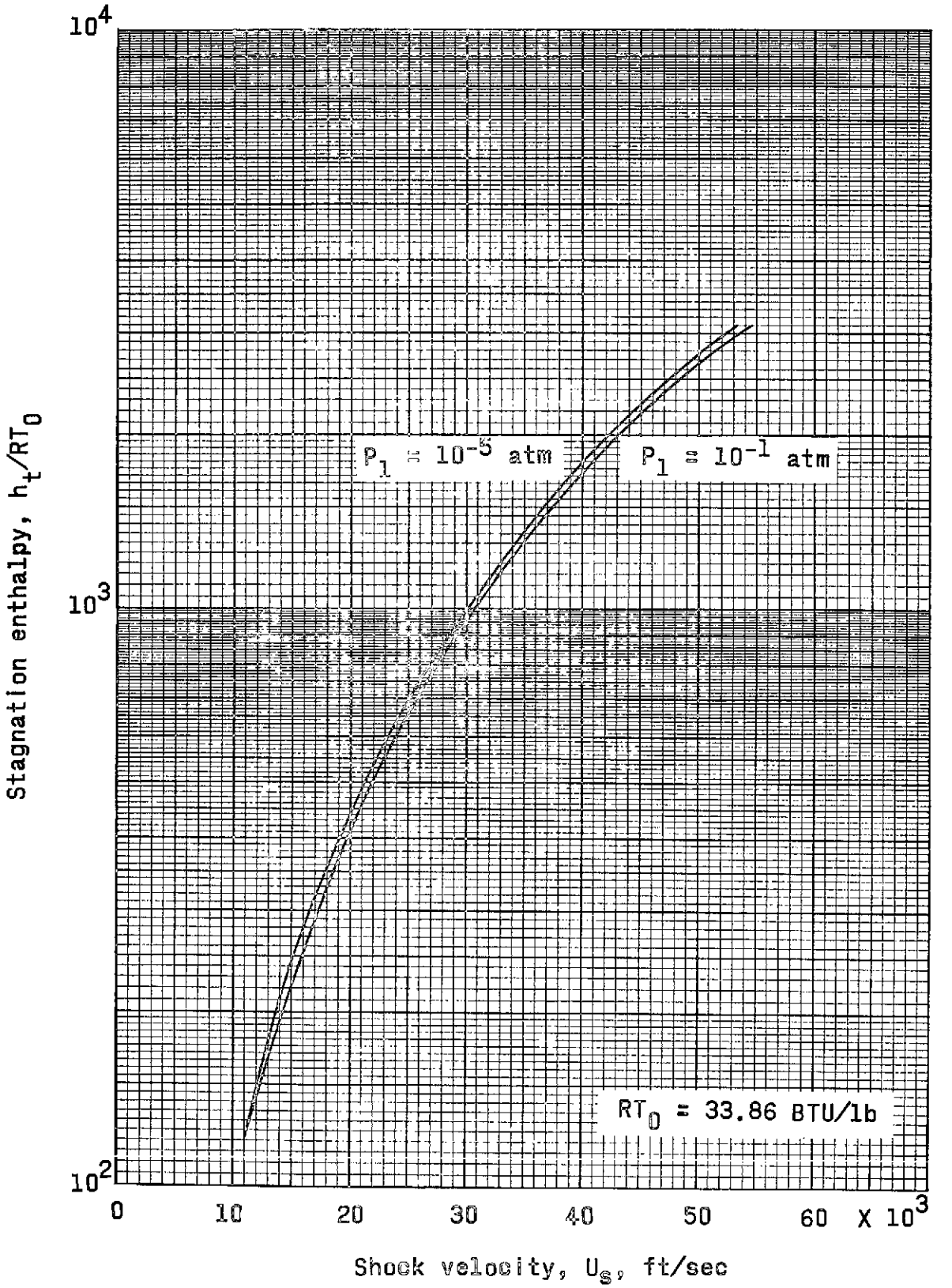

Figure 19.- Stagnation enthalpy of test gas vs shock velocity.

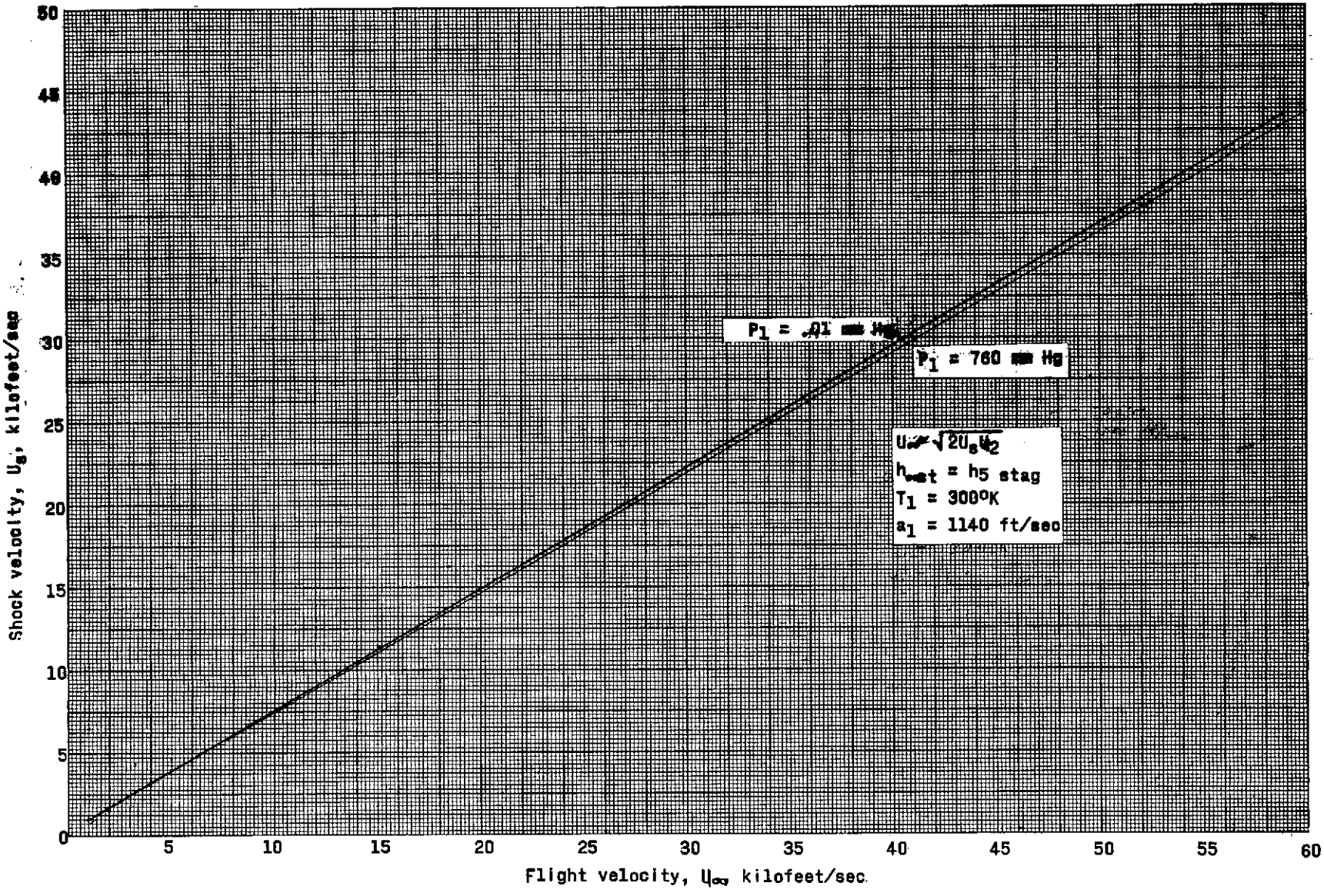

Figure 20.- The shock velocity for stagnation entholpy simulation versus the flight velocity.

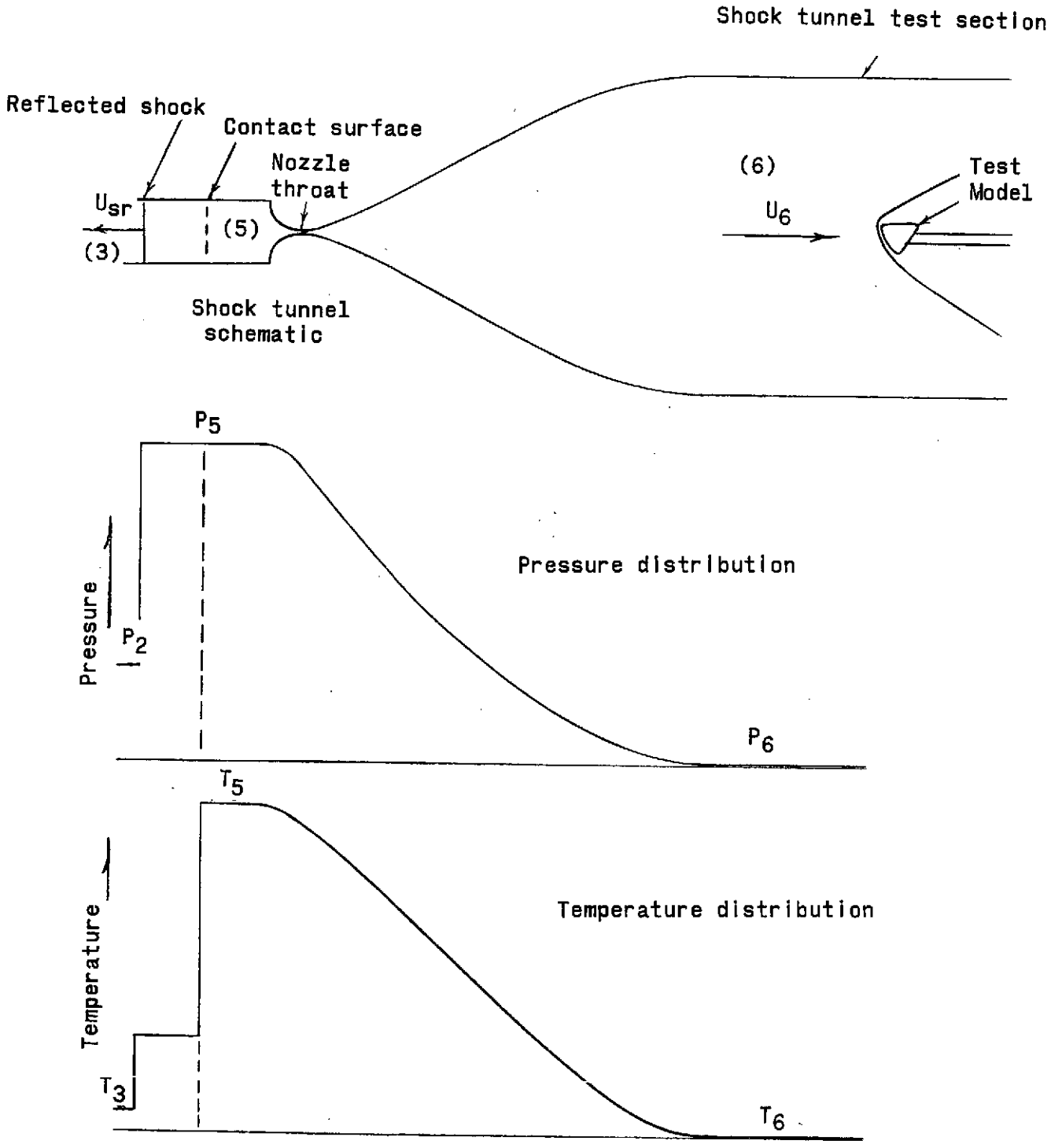

Figure 21.- Shock tunnel schematic and illustrative pressure and temperature distributions.

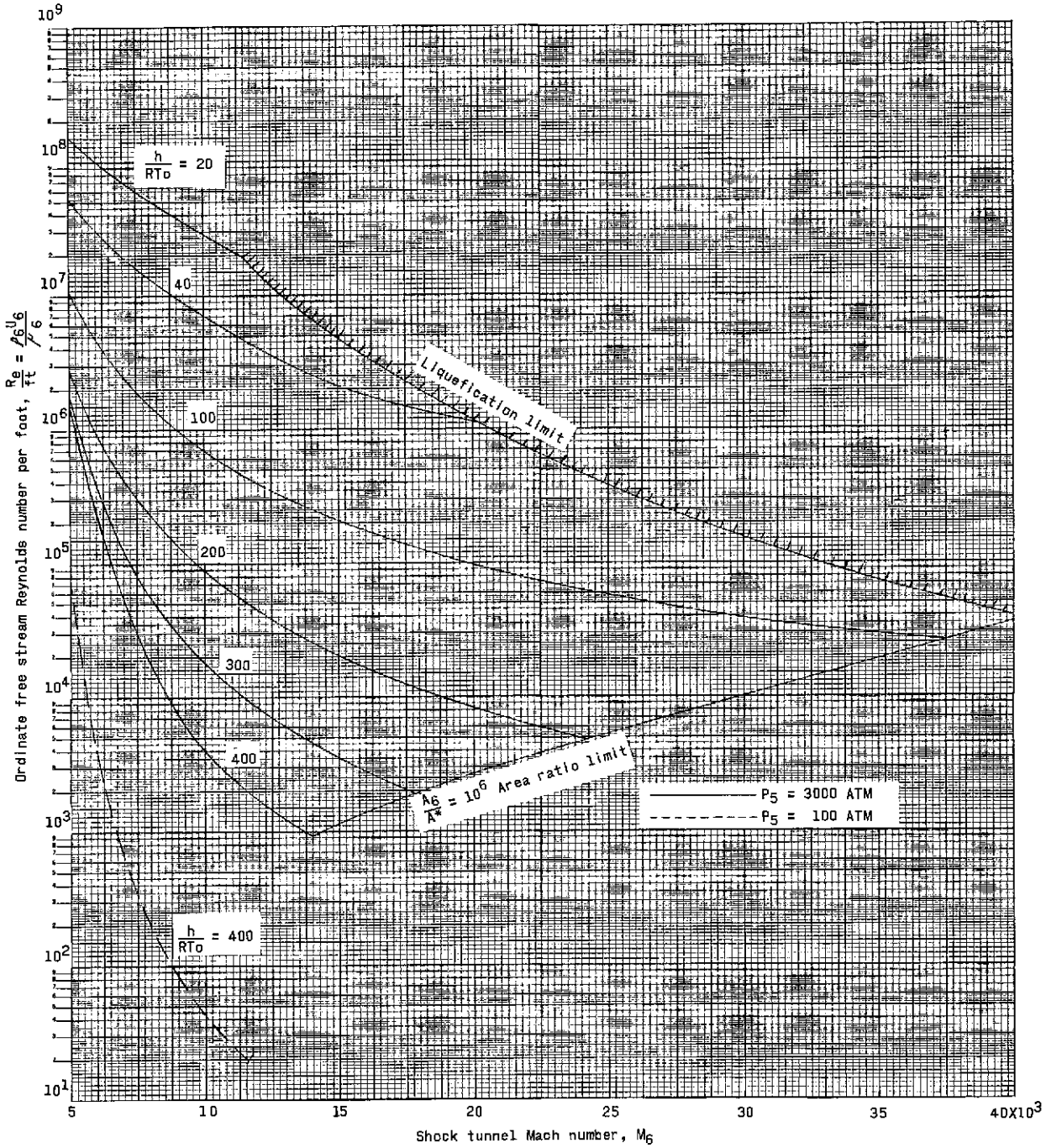

Figure 22.- Reynolds number, Mach number performance range for a hypersonic shock tunnel.